The Aeronautical Journal (2024), **128**, pp. 2604–2633
doi:10.1017/aer.2024.93

RESEARCH ARTICLE

Impact of operator characteristics on landing gear ground manoeuvre occurrences

J. Hoole, J.D. Booker and J.E. Cooper

Faculty of Engineering, University of Bristol, Bristol, UK
Corresponding author: J. Hoole; Email: josh.hoole@bristol.ac.uk

Received: 22 November 2023; **Revised:** 26 April 2024; **Accepted:** 19 August 2024

Keywords: Aircraft Trajectories; Landing Gear; ADS-B; Fatigue; Data Analytics

Abstract

The variability in ground manoeuvre occurrences for aircraft landing gear is intrinsically linked to the airport geometries served by aircraft in-service and consequently, the cyclic loads that landing gear carry are driven by the route network and characteristics of aircraft operators. Currently, assumptions must be made when deriving fatigue load spectra for aircraft landing gear, which may fail to capture the operator characteristics, potentially leading to design conservatism. This paper presents the enhanced characterisation of ground turning manoeuvres within the Automatic Dependent Surveillance-Broadcast (ADS-B) trajectories for six narrow-body aircraft across a full-service carrier (FSC) and a low-cost carrier (LCC) fleet. The methodology presented within this paper employs ADS-B latitude and longitude information to overcome limitations of previous approaches, increasing the rate of correct manoeuvre identification within ADS-B trajectories to 77% of flights from the 50% rate achieved previously. When characterising the ground manoeuvres across 3,000 flights, significant differences in manoeuvre occurrences were observed between individual aircraft within the LCC fleet and between the FSC and LCC fleets. The occurrence of tight and pivot turns were shown to vary across the six aircraft with six and eight fatigue-critical turns being performed by the FSC and LCC fleet for every 10 flights performed. In addition, it was observed that the direction of fatigue critical turns is biased in specific directions, suggesting that individual main landing gear assemblies will accumulate fatigue damage at an increased rate, leading to greater justification for operator-specific spectra and structural health monitoring of aircraft landing gear.

Nomenclature

ADS-B	automatic dependent surveillance-broadcast
FAA	Federal Aviation Administration
FSC	full service carrier
GPS	Global Positioning Systems
LCC	low-cost carrier
N_T	total number of taxi turns
R_{avg}	average estimated turn radius
ULCC	ultra-low-cost carrier

Greek symbol

α	bearing between two ADS-B position reports
$\Delta\alpha$	change in bearing between three consecutive ADS-B position reports
Δd	distance between two ADS-B position reports

This paper is a version of a presentation given at the 8th Aircraft Structural Design Conference held in October 2023.

https://doi.org/10.1017/aer.2024.93 Published online by Cambridge University Press

Δt	time between two ADS-B position reports
$\Delta\theta_{s,max}$	maximum spatial turn rate observed during turn

1.0 Introduction and background

Within the fatigue design of aircraft landing gear, the various cyclic loads that the landing gear is subjected to during taxi must be accounted for within the assumed loading spectrum [1–3]. Such spectra must account for the occurrence and repetition of different types of ground manoeuvre (e.g. turns, pivoting and braking) along with the loading magnitude associated with each manoeuvre [4–6].

Prior work has highlighted that there is significant variability within ground manoeuvres performed by civil aircraft in-service, both in terms of manoeuvre occurrence [6] and loading magnitude [7]. However, the current construction of load spectra during landing gear fatigue design requires assumptions to be made regarding the occurrence of ground manoeuvres and are also typically based on average values of ground manoeuvre occurrences, rather than representing the full variability in manoeuvre occurrence [3, 6, 8, 9]. Such assumptions in load spectra need to be validated and challenged to support the design of more efficient landing gear assemblies which also retain their structural integrity in-service.

The source of the variability in landing gear ground manoeuvre occurrences is the taxi routes that aircraft perform at airports. Such taxi routes vary from flight-to-flight due to airport geometry, active runway direction, local air traffic procedures and the aircraft operator's typical gate/stand locations [6]. As a result, the ground manoeuvres an aircraft performs are inherently tied to the aircraft operator, as this dictates the route network for the aircraft along with parking locations at departure and arrival airports.

Recently, trajectories from in-service aircraft derived from air traffic data have been used to identify the significant variability in the ground manoeuvres of the global fleet of wide-body aircraft [6]. This paper intends to extend this prior work through exploring the feasibility of tracking individual aircraft ground manoeuvres over a series of consecutive flights, in order to assess the airframe-level ground manoeuvre variability, along with comparing how ground manoeuvre occurrences vary between different aircraft operators. Through better understanding the ground manoeuvres performed by individual operators, it is proposed that dedicated and better-informed fatigue load spectra could be defined, potentially reducing the conservatism present in existing spectra. A challenge of the conservatism could lead to future structural assemblies with reduced mass or longer service life [10]. Such an investigation will also provide data and results that can support the growing interest in the structural health monitoring of individual landing gear assemblies [3, 11–18].

2.0 Landing gear ground manoeuvre occurrence identification methodology

The exploitation of 'real-time' and historic aircraft trajectories derived from crowd-sourced air traffic data has become a significant tool across the research areas of airborne and ground air traffic management [19, 20], aircraft emissions [21] and aerospace system design [6]. The most common source of air traffic data is automatic dependent surveillance-broadcast (ADS-B) transmissions, now mandated in many civil aircraft [22], which provides aircraft position reports (latitude, longitude and altitude) at a maximum frequency of two broadcasts a second [23]. When captured by ground-based receivers and collated into repositories such as Flightradar24 [24] and the OpenSky Network [25], historic ADS-B trajectories for individual aircraft and flights are then available. Due to the reliance of ground-based receivers, each repository has differing levels of coverage for airport ground operations. In addition, the temporal resolution of datasets from different ADS-B repositories can vary due to differing data processing and storage approaches. ADS-B data can also contain positional errors as discussed by Ali et al. [26].

Within the focus of aerospace fatigue design and structural health monitoring, ADS-B has previously been employed to characterise the variability in training helicopter manoeuvres [27], provide health monitoring of helicopter gearboxes [28] and to characterise the variability in wide-body aircraft landing gear ground manoeuvres [6]. There is also the future ambition to explore the use of remote sensing of

https://doi.org/10.1017/aer.2024.93 Published online by Cambridge University Press

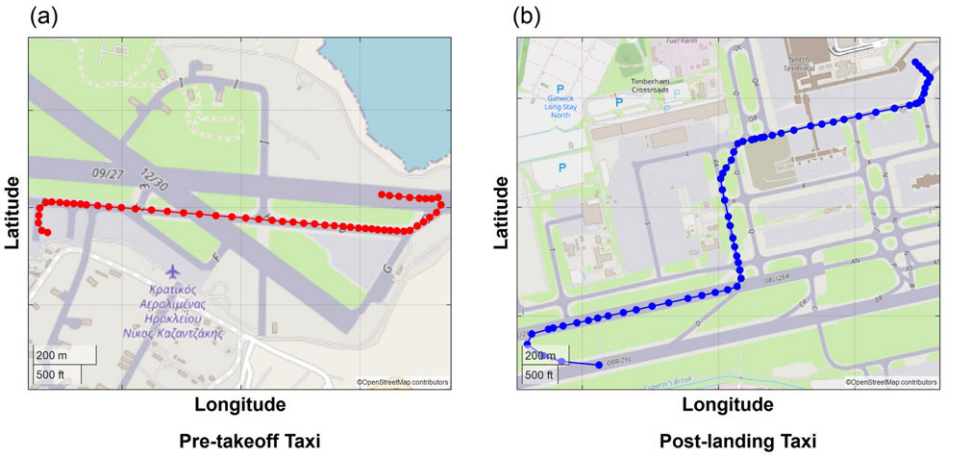

Figure 1. *Example of (a) pre-takeoff and (b) post-landing taxi routes from ADS-B trajectories. ADS-B data from Flightradar24 [24]. Map data from OpenSteetMap (https://www.openstreetmap.org/copyright).*

airframe accelerations and loads via ADS-B to support structural health monitoring of aircraft structures [29, 30].

An example of the taxi routes derived from an ADS-B trajectory is shown in Fig. 1 for the pre-takeoff taxi at the departure airport and the post-landing taxi at the arrival airport. It can be observed from Fig. 1 that there are sufficient ADS-B transmission data points to visually identify the taxi routes, from pushback to runway entry and runway exit to the final turn onto stand.

As shown in Fig. 1, ADS-B trajectories can provide sufficient resolution of the aircraft taxi route performed during a flight to manually and visually identify the ground manoeuvres performed. Prior work has detailed a framework and rule-based methodology to automatically identify aircraft ground manoeuvres from ADS-B trajectories [6]. The existing methodology identifies the changes in aircraft track angle and speed between consecutive ADS-B transmissions and through a series of conditional statements and grouping of consecutive identical changes in the aircraft trajectory extracts, turning and deceleration manoeuvres [6].

However, a number of limitations of the algorithm were identified previously, along with their proposed mitigation [6]. A significant limitation highlighted was the reliance on aircraft track for identifying turn direction, especially where ADS-B data was intermittent, missing or noisy and the use of latitude and longitude information was proposed as an alternative [6]. Characterisation of ground turning manoeuvres is of vital importance within landing gear fatigue design, as the lateral and torsional loads applied during turns are considered fatigue-critical design conditions [8]. Therefore, inclusion of 'tight' or pivoting turns into the fatigue spectra is especially important, along with turn 'reversals' (e.g. a left turn immediately followed by a right turn), due to their increased cyclic loading magnitudes [1, 4, 6]. Consequently, exploration of how ground turn characterisation from ADS-B trajectories can be enhanced, both in terms in robustness and extracted information was considered.

2.1 Enhanced turn manoeuvre characterisation

Within the ADS-B trajectory for a given flight, the aircraft's latitude and longitude position will be reported during the taxi phase, as shown previously in Fig. 1. Between two consecutive ADS-B transmissions, the bearing and distance between the two aircraft positions, as defined using GPS latitude and longitude, can be computed. The definition of the bearing between two latitude and longitude positions is shown in Fig. 2.

https://doi.org/10.1017/aer.2024.93 Published online by Cambridge University Press

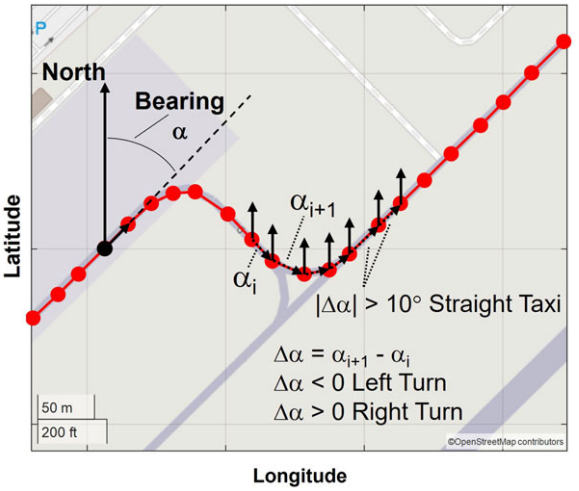

Figure 2. *Definition of bearing between ADS-B trajectory points and turn direction identification. ADS-B data from Flightradar24 [24]. Map data from OpenSteetMap (https://www.openstreetmap.org/copyright).*

Rather than relying on the reported aircraft track, the change in the bearing between three sets of consecutive latitude and longitude positions are used to identify if a left or right turn is being performed, as shown in Fig. 2. The ADS-B ground trajectory is then worked through, point-by-point, and consecutive positions with the same turning direction are grouped together. Any identified turns $< 10°$ were assumed to be positions of straight taxiing, as prior work demonstrated that deviations of up to 2° were observed during straight taxiing [6]. In addition, airport geometries typically employ taxiway turns of 30°, 45°, 60°, 90°, 120°, 135° and 150° [31], resulting in the selection of a $> 10°$ turn threshold providing discrimination between straight taxiways and typical taxiway turn angles. ADS-B trajectories have been shown to demonstrate significant noise when the aircraft is stationary [6] and consequently, zero-speed trajectory points are also removed from the dataset.

The use of latitude, longitude and bearing information, rather than the reported aircraft heading to identify turn direction also permits two limitations of the prior algorithm to be overcome. Firstly, the original track-based algorithm could identify 'false' turns due to noisy ADS-B data, where the aircraft would rapidly jump to another taxiway location, prior to returning to the actual ground trajectory (see Fig. 3) [6]. In order to filter out such occurrences, the distance between consecutive latitude and longitude positions were compared to the expected distance travelled by the aircraft based on its current ground speed. Any ADS-B position reports with a disagreement greater than a factor of 2 between the observed and estimated distances was removed from the trajectory.

The prior algorithm also failed to identify S-turn reversals when there were insufficient ADS-B trajectory data points to map out the two consecutive turns (see Fig. 4) [6]. Therefore, it was defined that if a turn was identified via bearing change between two latitude and longitude positions and that the bearing change between the preceding and following straight taxi elements was $< 10°$ that an S-turn had been performed, as shown in Fig. 4.

Finally, the bearing change between latitude and longitude positions was employed to identify the end of the aircraft pushback. Manual identification of pushbacks within trajectories highlighted that the end of the pushback would be marked by a single bearing change between consecutive latitude and longitude positions in excess of 60°, as shown in Fig. 5. As a result, the single ADS-B trajectory point in the pre-takeoff taxi phase displaying such a bearing change was marked as the pushback apex, and any turning manoeuvres preceding the pushback apex were relabelled as turns occurring during pushback.

https://doi.org/10.1017/aer.2024.93 Published online by Cambridge University Press

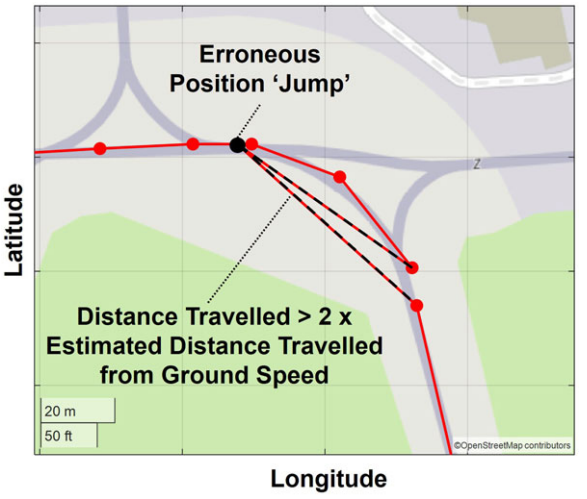

Figure 3. *Example of an erroneous ADS-B trajectory position. ADS-B data from Flightradar24 [24]. Map data from OpenSteetMap (https://www.openstreetmap.org/copyright).*

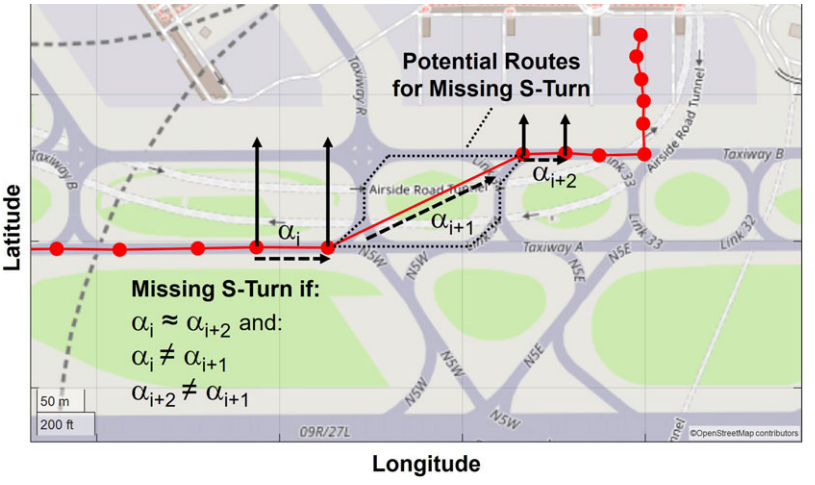

Figure 4. *S-turn identification with missing ADS-B trajectory positions. ADS-B data from Flightradar24 [24]. Map data from OpenSteetMap (https://www.openstreetmap.org/copyright).*

2.1.1 Characterisation of tight and pivot turns

As highlighted in Section 2, landing gear ground turning manoeuvres must be characterised into normal taxiway turns and those involving 'tight' or 'pivot' turns, in which typically the aircraft will turn with one of the main landing gear remaining near stationary [1, 4]. The transition to identifying turns via latitude and longitude position changes permitted additional parameters relating to each turn to be computed, as visualised in Fig. 6:

- Mean and maximum temporal turn rate (deg/s)
- Mean and maximum spatial turn rate (deg/m)

https://doi.org/10.1017/aer.2024.93 Published online by Cambridge University Press

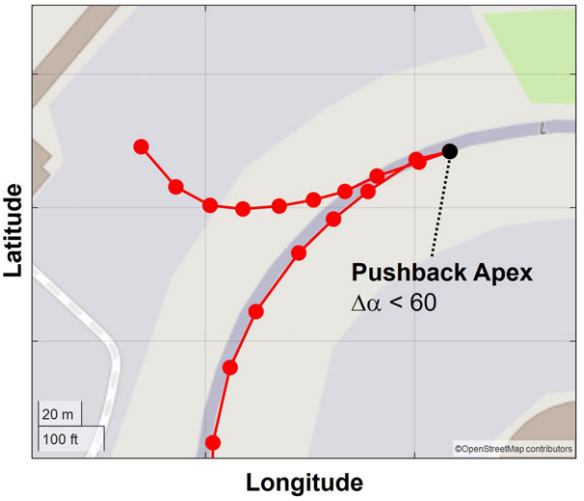

Figure 5. *Identification of pushback apex. ADS-B data from Flightradar24 [24]. Map data from OpenSteetMap (https://www.openstreetmap.org/copyright).*

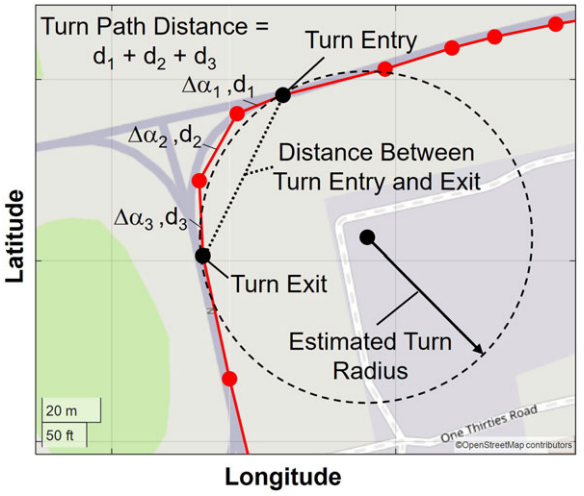

Figure 6. *Definition of turn characteristics. ADS-B data from Flightradar24 [24]. Map data from OpenSteetMap (https://www.openstreetmap.org/copyright).*

- Turn radius estimated via turn path distance (m)
- Turn radius estimated via distance between turn entry and exit (m)

The radius of a turn could be approximated through assuming that all turns took a circular profile, and the computed distance represented the fraction of the circumference in the same ratio as the total turn angle to 360°. It was found that estimating the radius via turn path distance was suitable for turns with multiple ADS-B trajectory points and typically of 90°, whilst the radius estimation via the entry-exit distance was required for small angle turns or those without a large number of reported positions. Therefore, the average estimated turn radius was also computed using the turn path and entry and exist distance values.

https://doi.org/10.1017/aer.2024.93 Published online by Cambridge University Press

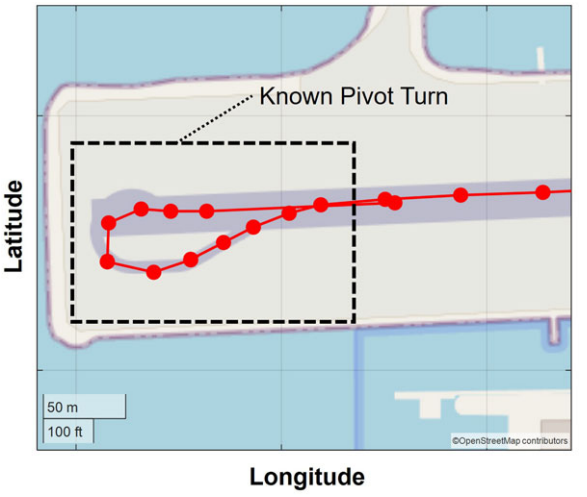

Figure 7. *Example of a known pivot turn. ADS-B data from Flightradar24 [24]. Map data from OpenSteetMap (https://www.openstreetmap.org/copyright).*

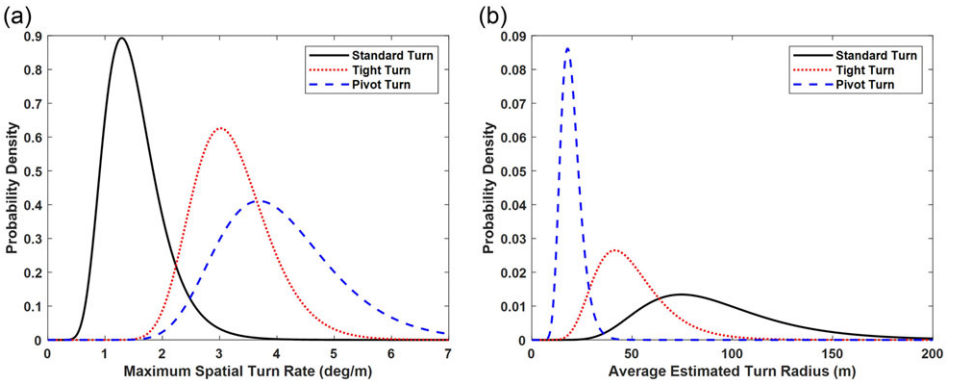

Figure 8. *Variability in (a) maximum spatial turn rate and (b) average estimated turn radius R_{avg} for standard, tight and pivot turns.*

In order to automatically characterise tight and pivot turns within the ADS-B trajectories, 20 ADS-B trajectories containing the following manoeuvres, known to result in tight turns, were selected and the turn parameters computed for each relevant turn:

- Runway pivot turns after runway backtrack (see Fig. 7)
- Tight runway entry turns (typically as the final element of a standard taxiway turn)
- Tight turn onto stand manoeuvres

The variability in each of the turn parameter values was characterised using a Log-Normal distribution due to the observed right-tail skew in the values and potential for zero-thresholds for pivot turn radii and near-zero turn rates for shallow/wide turns. The turn parameters that provided the greatest separation between standard, tight and pivot turns were found to be the maximum spatial turn rate '$\Delta\theta_{s,max}$' and average estimated turn radius 'R_{avg}', as shown by the distributions in Fig. 8.

https://doi.org/10.1017/aer.2024.93 Published online by Cambridge University Press

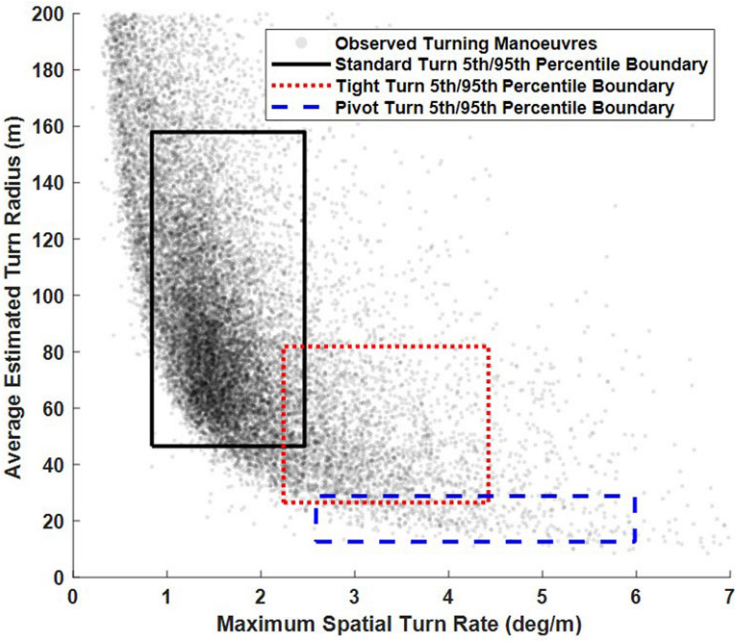

Figure 9. *Regions for known standard, tight and pivot turns based upon* 5th *and* 95th $\Delta\theta_{s,max}$ *and* R_{avg} *percentiles.*

Employing the 5th and 95th percentiles of each distribution permitted definition of the turn characterisation space shown in Fig. 9. For example, the bounding box for tight turns shown in Fig. 9 is given by the percentile values derived from the Log-Normal distributions:

- $\Delta\theta_{s,\max}$ 5th Percentile value: 2.24deg/m
- $\Delta\theta_{s,\max}$ 95th Percentile value: 4.43deg/m
- R_{avg} 5th Percentile value: 26.5m
- R_{avg} 95th Percentile value: 81.9m

Figure 9 also shows all of the turns extracted from the flights of one of the aircraft described in Section 3. It can be observed that there is overlap in some of the turn characteristic regions, along with undefined regions. Consequently, the turn characterisation space was simplified, assuming the boundaries between overlapping regions were set at the mid-point of the overlap, along with extending any regions to the minimum and maximum axis position. This simplification resulted in the characterisation space shown in Fig. 10 and the turn characterisation conditional statements shown in Equation (1).

$$\text{TurnType} = \begin{cases} \text{NormalTurn} & \text{if} \Delta\theta_{s,max} \leq 2.33\text{deg/m} \\ \text{TightTurn} & \text{if} \Delta\theta_{s,max} > 2.33 deg/m and R_{avg} > 27.5m \\ \text{PivotTurn} & \text{if} \Delta\theta_{s,max} > 2.33 deg/m and R_{avg} \leq 27.5\text{m} \end{cases} \quad (1)$$

3.0 Dataset collection

Airline operations can be broadly split into two types, full-service carriers (FSCs) or low-cost carriers (LCCs) [32]. FSC operators are typically based at larger primary airports and operate hub-to-hub routes, with LCC operators focusing on secondary airports, typically operating point-to-point routes [32]. To explore the impact of these two operator characteristics on the ground manoeuvres performed by aircraft,

https://doi.org/10.1017/aer.2024.93 Published online by Cambridge University Press

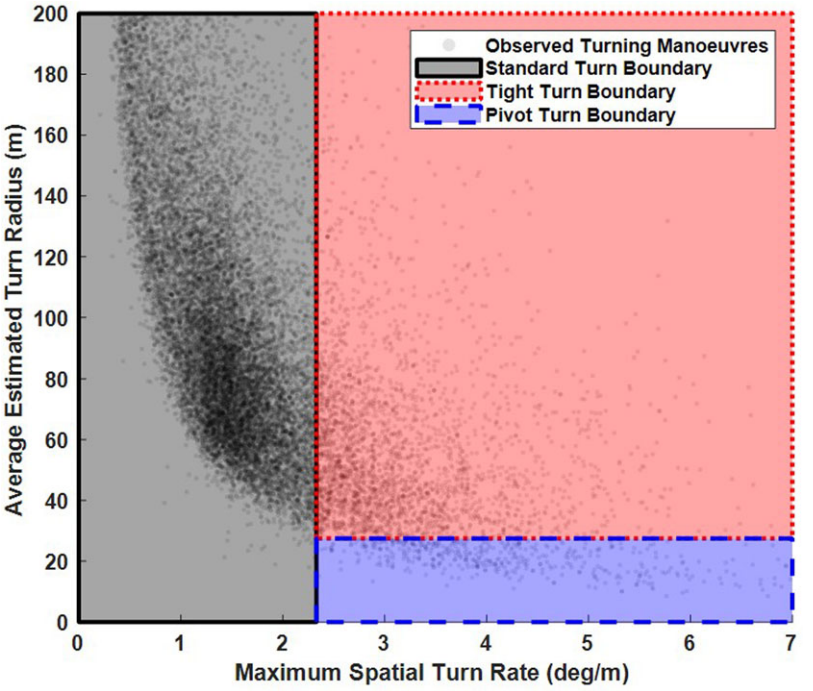

Figure 10. *Assumed $\Delta\theta_{s,max}$ and R_{avg} regions for standard, tight and pivot turns.*

three narrow-body aircraft from a European FSC operator fleet and three narrow-body aircraft from a European LCC fleet were identified. Narrow-body fleets were selected due to the perceived increase in route variability and to enable a comparison with the wide-body global fleet data captured previously [6]. The characteristics of each narrow-body aircraft within the data collection timeframe were as follows:

- **FSC 1:** aircraft consistently based at a large international airport
- **FSC 2:** aircraft consistently based at the same airport as FSC 1
- **FSC 3:** aircraft consistently based at the same airport as FSC 1
- **LCC 1:** aircraft based at two secondary international airports
- **LCC 2:** aircraft rotated around secondary international airports and regional airports
- **LCC 3:** aircraft rotated around two regional airports

The FSC fleet aircraft were selected to have the same base airport to permit the variability in ground manoeuvres resulting from solely the operator's route network to be identified. The results from the FSC fleet could then be compared to the LCC fleet, which were routinely rotated around the operator's bases and route network, permitting the impact on ground manoeuvre variability to be compared between the two operator types. Multiple aircraft within the LCC fleet were reviewed to ensure the different base characteristics within the LCC route network were captured, whilst the FSC aircraft were selected based on not having significant gaps within their utilisation as a result of being out of service.

For each individual airframe, ADS-B trajectories for 500 consecutive flights in the period of Summer-Autumn 2021 were sourced from Flightradar24 [24]. This period of time was employed to capture the potential increase in seasonal routes flown by the LCC operator and the year of 2021 was required due to the need to be able to select the LCC aircraft based upon their long-term fleet rotation strategy, which can only be apparent from reviewing historic aircraft operations retrospectively. Studies concerning the capture of ADS-B transmissions highlighted that during the latter half of 2021, ADS-B data collection

https://doi.org/10.1017/aer.2024.93 Published online by Cambridge University Press

Table 1. *Proportion of dataset containing taxi route elements*

Aircraft	Pushback	Pre-takeoff	Post-landing	Turn ontostand	Complete taxi
FSC 1	95.6%	88.8%	85.0%	88.2%	70.2%
FSC 2	93.2%	93.2%	91.0%	89.0%	77.6%
FSC 3	96.0%	91.8%	89.6%	86.7%	76.8%
FSC fleet	*94.9%*	*91.3%*	*88.5%*	*88.0%*	*74.9%*
LCC – large airport	87.8%	88.0%	87.6%	76.6%	61.0%
LCC – rotation	83.0%	88.4%	86.0%	73.4%	53.2%
LCC – regional	78.4%	87.0%	84.8%	59.8%	40.4%
LCC fleet	*83.1%*	*87.8%*	*86.1%*	*69.9%*	*51.5%*
Narrow body fleet	89.0%	89.5%	87.3%	79.0%	63.2%

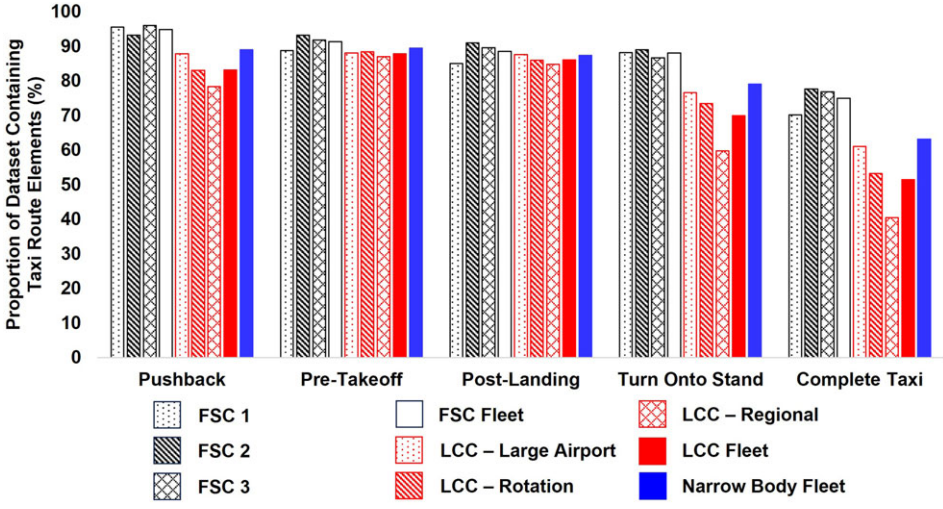

Figure 11. *Visualisation of proportion of dataset containing taxi route elements.*

rates had begun to recover after the COVID-19 pandemic [21]. The sample of size of 500 flights was selected to represent a typical time between aircraft maintenance checks [33], assuming that each flight cycle lasts 1.5 hours. Flightradar24 [24] was used as the ADS-B source due to its adequate coverage of ground operations at European airports.

3.1 ADS-B trajectory data quality

Prior to identifying the turning manoeuvres performed within the trajectories for each individual aircraft, the ADS-B trajectory data quality was first assessed by manually reviewing the 3,000 assembled flights. Each trajectory was visually checked to identify whether it contained sufficient ADS-B data points to identify the manoeuvres during pushback, pre-takeoff taxi, post-landing taxi and the turn onto stand.

The resulting proportions of flights containing ADS-B trajectories for the four taxi phases are shown in Table 1 and visualised in Fig. 11. When aggregating across all six aircraft, it can observed that approximately 80% of flights will contain pushback, taxi and turn onto stand trajectories, with approximately 60% of flights containing the full taxi route. This latter value represents an $\approx$ 10% increase in the number of flights with complete taxi trajectories compared to the dataset collected in 2019 for the wide-body aircraft study [6].

https://doi.org/10.1017/aer.2024.93 Published online by Cambridge University Press

Table 2. *Dataset resolution*

	Pre-takeoff		Post-landing	
Aircraft	Δt (s)	Δd (m)	Δt (s)	Δd (m)
FSC 1	19	44	8	45
FSC 2	14	46	7	46
FSC 3	19	44	8	44
FSC fleet	*17*	*45*	*8*	*45*
LCC – large airport	17	39	6	45
LCC – rotation	12	37	6	44
LCC – regional airport	13	40	6	46
LCC fleet	*14*	*39*	*6*	*45*
Narrow body fleet	16	42	7	45

From Table 1 and Fig. 11, it is also clear to see that the LCC aircraft have lower overall proportions for ADS-B trajectories containing taxi route elements and these proportions are seen to decrease as the airport size reduces from large international airports to regional airports. This especially concerns the availability of turn onto stand information for the LCC aircraft fleet, as 15% fewer flights contain turn onto stand information for the aircraft based exclusively at regional airports, compared to the FSC fleet. It is anticipated that such an observation is due to there being fewer ADS-B ground receivers installed close to smaller airports.

The ADS-B trajectories were also assessed for their temporal and spatial resolution. For each of the 3,000 available flights, the time difference 'Δt' and distance between the latitude and longitude 'Δd' for each consecutive ground trajectory point were computed, and the average values for each aircraft and fleet are shown in Table 2.

It can be observed that the average timestep between ADS-B trajectories for both pre-takeoff and post-landing is significantly higher than the minimum ADS-B specification of 0.5 seconds [23]. This effect is anticipated to be due to the dataset compression typically performed by ADS-B repositories, along with removal of zero-speed trajectories elements as described in Section 2.1. This finding also supports the results in Table 2 which demonstrate that the temporal resolution is doubled for the post-landing taxi phase compared to the pre-takeoff taxi phase. During peak operational times, it has been observed that aircraft queue at runway hold points [6], and this will lead to an increased prevalence of zero-speed trajectory elements within the pre-takeoff taxi phase. The increased temporal resolution for regional airports shown in Table 2 also supports the trend of decreased temporal resolution for increased zero-speed trajectory elements, as such airports would be expected to have fewer instances of congestion.

Table 2 also demonstrates the spatial resolution of the ADS-B trajectories, and it can be observed that the average distance between ADS-B position reports is of similar magnitude to the fuselage length and wingspan of a narrow-body aircraft [34, 35]. This observation further supports the adoption of latitude and longitude based manoeuvre identification due to the high average spatial resolution achieved and further supports the adoption the spatial turn parameters $\Delta\theta_{s,max}$ and R_{avg} for characterising turn types.

3.2 Verification of manoeuvre identification methodology

The enhanced turn manoeuvre characterisation methodology described in Section 2 also required verification prior to characterising the manoeuvres in the ADS-B trajectories of the six aircraft. For verification, 10% of the dataset (i.e. 50 flights per airframe) were assessed using the methodology, along with the manual characterisation of the taxi route and turns through plotting the ADS-B trajectory in reference to airport geometries (as shown previously in Fig. 1). Table 3 shows the proportion of flights for which the algorithm correctly identified the pre-takeoff taxi, post-landing taxi and complete ground trajectories. It can be observed that in nearly 80% of individual flights the correct ground manoeuvres were

https://doi.org/10.1017/aer.2024.93 Published online by Cambridge University Press

Table 3. *Verification of manoeuvre identification*

	Flights with correct manoeuvre identification		
Aircraft	Pre-takeoff	Post-landing	Whole flight
FSC 1	72%	90%	62%
FSC 2	90%	96%	86%
FSC 3	88%	90%	80%
FSC fleet	*83%*	*92%*	*76%*
LCC – large airport	88%	90%	78%
LCC – rotation	86%	90%	78%
LCC – regional airport	86%	88%	76%
LCC fleet	*87%*	*89%*	*77%*
Narrow body fleet	85%	91%	77%

identified in the pre-takeoff and post-landing taxi phases. This value represents a significant increase in the ≈50% success rate of the heading-based turn identification algorithm [6], justifying the adoption of turn characterisation via ADS-B latitude and longitude positions.

Whilst the vast majority of values in Table 3 are consistent across the aircraft and fleets, it is important to note that processing of FSC 1 trajectories showed degraded accuracy for the pre-takeoff taxi phase. As this aircraft was based at the same airport as FSC 2 and FSC 3, it suggested that FSC 1 may have been operating on routes with increased levels of noise within the ADS-B trajectory, leading to increased rates of erroneous manoeuvre identification.

4.0 Results

This section will present and discuss the results from applying the ground manoeuvre characterisation algorithm to the 500 flights associated with each airframe, in order to establish how the FSC and LCC operator characteristics impact the ground manoeuvres performed by the aircraft and the landing gear load spectrum.

4.1 Pre-takeoff taxi

The histograms shown across Fig. 12 show the variability in the number of pre-takeoff turns and taxi distance across the FSC and LCC fleets. As can be observed from Fig. 12(a), both the FSC and LCC narrow-body fleets have a mode number of pre-takeoff turns equal to four, which is in good agreement with the mode and median turn values identified for a global wide-body aircraft fleet [6] and average turn occurrence of four [34] and six [35] from the Federal Aviation Administration (FAA) statistical loads data for narrow-body aircraft. It can be observed from Fig. 12(a) that the LCC fleet have a higher proportion of flights where the number of turns is below the mode value compared to the FSC fleet, and this is expected to be due to simpler airport geometries at smaller airports.

The histograms for taxi distances shown in Fig. 12(b) highlight a significant difference between the FSC and LCC fleet, whereby the FSC fleet demonstrates bi-modal variability with a high proportion of flights with a $>$ 3km pre-takeoff taxi. Increased taxi-distances may lead to increased occurrences of aircraft braking and vertical 'bump' loads over taxiway surfaces and hence are of interest during the construction of fatigue spectra [1, 4].

Concerning the three aircraft within the FSC fleet, it can be observed that the variability in pre-takeoff turns and taxi distance are consistent across the FSC fleet in Fig. 12(c) and (d). This observation aligns with the fact that the three FSC aircraft were based at the same international airport.

However, when reviewing the pre-takeoff histograms for the LCC aircraft in Fig. 12(e) and (f) it can be seen that there are differences in the mode number of pre-takeoff turns, the variability in the

https://doi.org/10.1017/aer.2024.93 Published online by Cambridge University Press

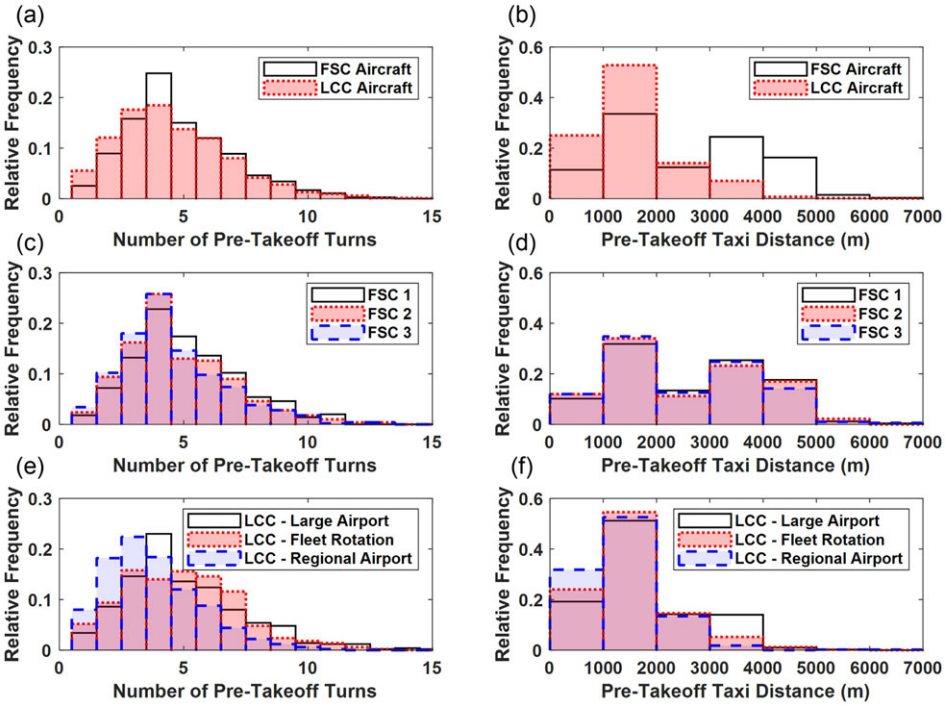

Figure 12. *Pre-takeoff taxi statistics: fleet-level (a) turn occurrences and (b) taxi distances, full-service carrier (c) turn occurrences and (d) taxi distances and low cost carrier (e) turn occurrences and (f) taxi distances.*

turn occurrence and the taxi distance. Figure 12(e) demonstrates that, as expected, the LCC aircraft operating from regional airports carries out fewer pre-takeoff turns compared the LCC aircraft based at large airports, with the mode values of three and four turns, respectively. The impact of rotating an aircraft around bases and the route network can also be observed from Fig. 12(e), leading to the variability in the number of pre-takeoff turns capturing the variability characteristics of both the large airport and regional airport LCC aircraft. The pre-takeoff taxi distances shown in Fig. 12(f) also show the expected response of the LCC aircraft based at the large airport presenting longer taxi distances compared to the regional airport-based aircraft.

Consequently, Fig. 12 has demonstrated that airport base, regardless of operator, has a significant impact on both the pre-takeoff turn occurrences and taxi distance, potentially leading to increased cyclic loading occurrences in aircraft based at larger airports, through increased mode number of turns and taxi distance.

4.1.1 Turn characteristics

As highlighted in Section 2.1.1 the characteristics of each pre-takeoff turn are required to inform future landing gear fatigue spectra guidelines. The proportion of the 'N_T' total number of turns extracted in the 500 flights of each aircraft displaying different turn type characteristics are shown in Table 4 and the standard, tight and pivot turn proportions are visualised in Fig. 13. From Table 4 it can be observed that across the aircraft of the FSC and LCC fleets, there is an equal share between left and right turns in the pre-takeoff taxi phase, consistent with the turn direction proportions observed previously for a wide-body aircraft [6].

https://doi.org/10.1017/aer.2024.93 Published online by Cambridge University Press

Table 4. *Pre-takeoff turn characteristics*

Aircraft	N_T	Left	Right	Standard	Tight	Pivot
FSC 1	2,399	50.4%	49.6%	87.0%	10.5%	2.5%
FSC 2	2,526	51.1%	48.9%	87.4%	10.0%	2.6%
FSC 3	2,236	51.9%	48.1%	87.8%	9.7%	2.5%
FSC fleet	*7,161*	*51.1%*	*48.9%*	*87.4%*	*10.1%*	*2.5%*
LCC – large airport	2,447	50.9%	49.1%	84.1%	12.8%	3.1%
LCC – fleet rotation	2,368	52.0%	48.0%	81.6%	15.8%	2.6%
LCC – regional airport	1,815	48.5%	51.5%	77.5%	18.8%	3.7%
LCC fleet	*6,630*	*50.5%*	*49.5%*	*81.1%*	*15.8%*	*3.1%*
Narrow body fleet	13,791	50.8%	49.2%	84.2%	13.0%	2.8%

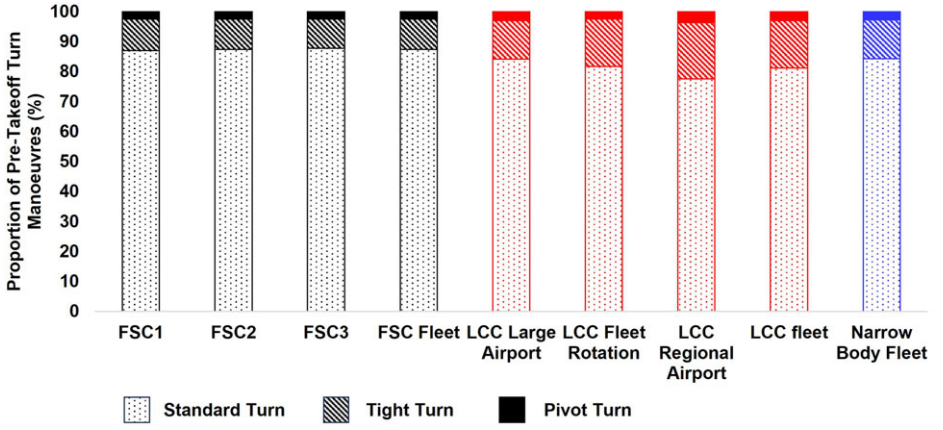

Figure 13. *Proportion of pre-takeoff turn types.*

Concerning the distribution of turns between standard, tight and pivot turns during the pre-takeoff taxi phase, it can be observed from Table 4 and Fig. 13 that it is expected that LCC fleets will perform a greater proportion of tight/pivot turns in-service, with ≈80% of turns being standard taxiway turns, compared to the FSC fleet, in which 87% of turns are normal taxiway turns. When considering that both the FSC and LCC fleet demonstrate that same mode number of pre-takeoff turns (see Fig. 12(a)) it is inferred that LCC fleets will perform a greater number of fatigue-critical tight and pivot turns. Whilst the proportions shown in Table 4 may infer that the LCC aircraft based exclusively at the regional airport will perform an increased number of tight and pivot turns, it must be noted that the absolute number of turns that the LCC aircraft based at regional airports performed was three quarters that of the LCC aircraft based exclusively at large airports, meaning that across the 500 observed flights for each aircraft, both performed approximately 400 tight or pivot turns.

The results in Table 4 and Fig. 13 highlight that 'tight' turns (i.e. where a small turn radius is achieved as part of larger turn radius, such as during runway entry and line-up) are significantly more common than pivot turns, and this is to be expected as pivot turns typically occur during runway backtrack at smaller airports [6]. Table 4 and Fig. 13 also demonstrate the expected trend of increasing number of tight and pivot turns as the airport size decreases.

Further investigation into the turn direction for the observed tight and pivot turns resulted in the proportional turn direction values shown in Table 5. For the FSC fleet, it can be seen that pivot turns are biased towards the right hand direction, and for the LCC aircraft operating at the large and regional airports that the tight turns are also biased towards right turns. This observation is important from

https://doi.org/10.1017/aer.2024.93 Published online by Cambridge University Press

Table 5. *Pre-takeoff tight turn characteristics*

Aircraft	Tight left	Tight right	Pivot left	Pivot right
FSC 1	47.8%	52.2%	33.3%	66.7%
FSC 2	55.3%	44.7%	49.2%	50.8%
FSC 3	51.9%	48.1%	37.5%	62.5%
FSC fleet	*51.7%*	*48.3%*	*40.0%*	*60.0%*
LCC – large airport	38.0%	62.0%	43.4%	56.6%
LCC – fleet rotation	53.9%	46.1%	53.2%	46.8%
LCC – regional airport	38.7%	61.3%	46.3%	53.7%
LCC fleet	*43.5%*	*56.5%*	*47.6%*	*52.4%*
Narrow body fleet	47.6%	52.4%	43.8%	56.2%

Table 6. *Occurrence of pre-takeoff turn reversals*

Aircraft	Pre-takeoff turn reversal rate
FSC 1	30.6%
FSC 2	31.4%
FSC 3	29.6%
FSC Fleet	*30.5%*
LCC – large airport	33.0%
LCC – fleet rotation	33.4%
LCC – regional airport	29.8%
LCC fleet	*32.1%*
Narrow body fleet	31.3%

a fatigue substantiation perspective, as tight and pivoting turns induce significant torsional loads on the near-stationary main landing gear assembly (e.g. right-hand landing gear for a right-hand turn) [1, 4]. Consequently, bias of turn direction in tight and pivoting turns could lead to fatigue damage accumulating faster in individual main landing gear assemblies.

Finally, the proportion of pre-takeoff turns that demonstrated a turn-reversal (e.g. a left turn immediately followed by a right turn) was identified for each aircraft, and the results are shown in Table 6. It can be observed that across all aircraft and fleets, the proportion of turns resulting in a turn reversal was approximately 30% and this is consistent with the observed turn reversal rate for a wide-body aircraft fleet [6]. Consequently, it can be concluded that operator characteristics have no effect on the pre-takeoff turn reversal occurrences.

4.1.2 Pushback characteristics

As described in Section 2.1, the pushback sequence of the pre-takeoff taxi phase was segregated from the ADS-B ground trajectory. Figure 14(a) and (b) show that whilst the mode number of turns and pushback distance are consistent between the two operator fleets, the FSC aircraft based at larger, more complex airports, show a tendency towards longer pushback distances (by approximately one aircraft fuselage length) and an increased frequency of of pushback manoeuvres involving more than one turn. From Fig. 14(c) and (d) it can be observed that the proportion of tail-left to tail-right pushback turn directions is approximately equal for both the FSC and LCC fleets.

Regarding the individual aircraft within the FSC and LCC fleets, it can be observed across Fig. 14(e)–(h) that within each of the fleets, the pushback distances and number of turns are consistent between the aircraft. Consequently, the results shown in Fig. 14 show that the operator characteristic

https://doi.org/10.1017/aer.2024.93 Published online by Cambridge University Press

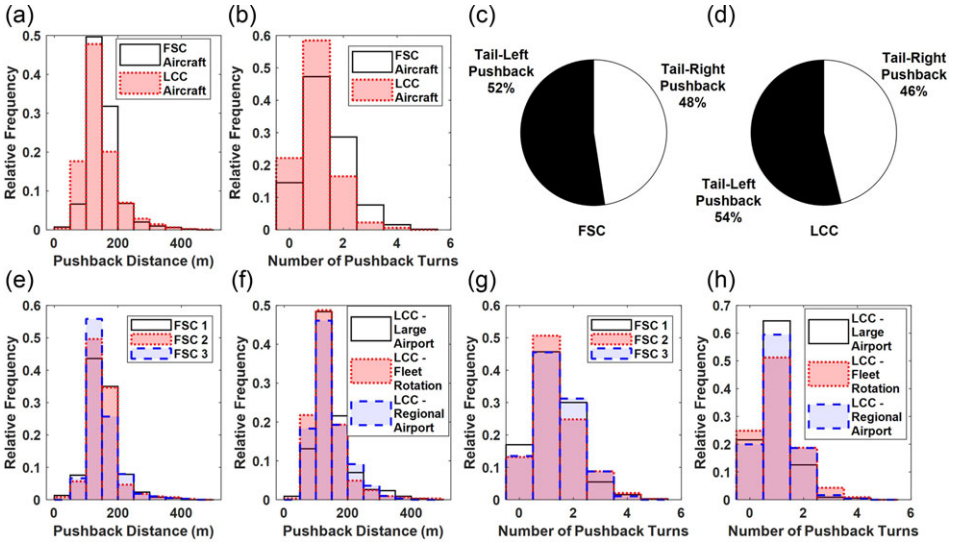

Figure 14. *Pushback statistics: fleet-level (a) pushback distance and (b) pushback turn occurrences, (c) full-service carrier and (d) low-cost carrier pushback turn direction proportion, (e) full-service carrier and (f) low-cost carrier pushback distances and (g) full-service carrier and (h) low-cost carrier pushback turn occurrences.*

and aircraft base have a lesser impact on the manoeuvres occurring pushback, when compared to the subsequent pre-takeoff taxi phase.

4.2 Post-landing taxi

Figure 15 shows histograms that capture the variability in the post-landing turning occurrences and taxi distance across the FSC and LCC fleets. Within Fig. 15(a), it can be observed that unlike the pre-takeoff turning cases, the mode number of post-landing turns differs between the FSC and LCC fleet, at four and three turns, respectively. These values are in good agreement with FAA statistical loads data for narrow-body aircraft, in which the average post-landing turn occurrence was four [34, 35]. It is interesting to note that the narrow-body fleet shows a higher mode number of post-landing turns compared to prior data from a wide-body aircraft fleet [6]. It is suggested that this may be due to the reduced post-landing ADS-B trajectory resolution observed in the previous study leading to the identification of fewer turns in the post-landing taxi phase. Ultimately, from comparing Figs. 12 and 15 it can be suggested that the mode number of turns for the narrow-body aircraft fleet is equal in the pre-takeoff and post-landing taxi phases.

Whilst Fig. 15(b) shows that a higher proportion of the FSC post-landing taxi distances are in excess of 2km compared to the LCC fleet, it should be noted that the difference between the post-landing taxi distances is reduced compared to the pre-takeoff taxi distances shown previously in Fig. 12(b). In addition, the bi-modal FSC taxi distance characteristic is also not apparent in the post-landing taxi phase.

An area of consistency between the pre-takeoff taxi phase and the post-landing taxi phase for the FSC aircraft is that the post-landing turn occurrences (see Fig. 15(c)) and taxi distances (see Fig. 15(d)) do not differ across the FSC fleet. However, the LCC fleet shows significantly different post-landing turn occurrences across the fleet, as shown in Fig. 15(e). As to be expected, the smaller regional airports result in fewer post-landing turns compared to the aircraft based at the larger airports. Once again, Fig. 15(e) demonstrates the impact of fleet rotation, with the LCC aircraft under fleet rotation spreading the turning occurrences across both the occurrence variability characteristics of the large and regional airport-based

https://doi.org/10.1017/aer.2024.93 Published online by Cambridge University Press

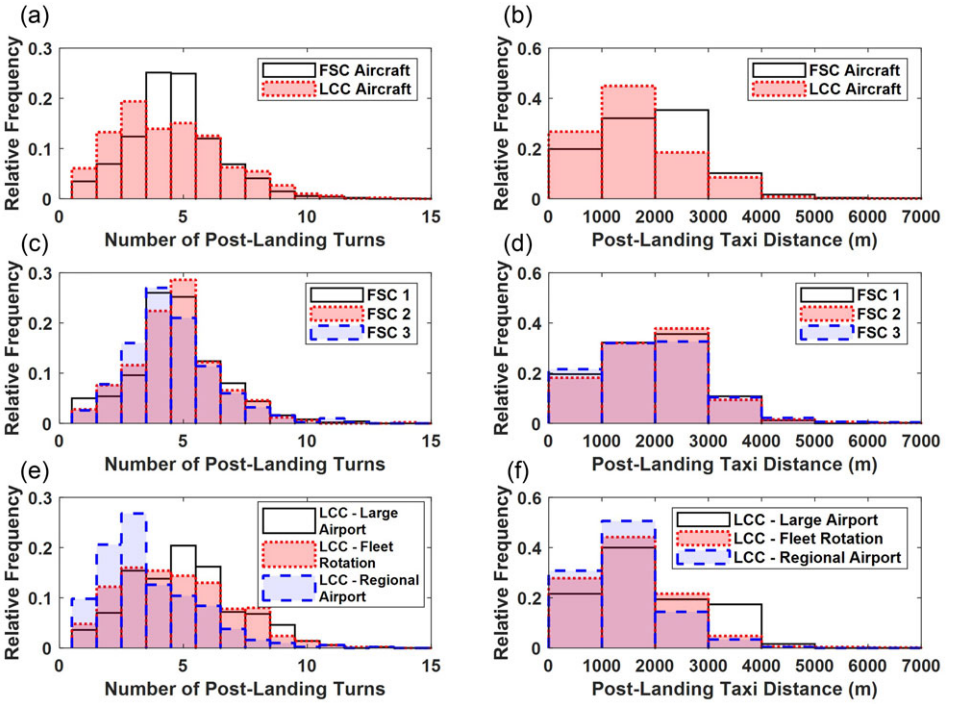

Figure 15. *Post-landing taxi statistics: fleet-level (a) turn occurrences and (b) taxi distances, full-service carrier (c) turn occurrences and (d) taxi distances and low-cost carrier (e) turn occurrences and (f) taxi distances.*

aircraft. As for the pre-takeoff taxi distance shown previously in Fig. 12(f), the LCC aircraft at large airports shows a higher proportion of flights with post-landing taxi distances $>$ 2km compared to the other LCC aircraft.

4.2.1 Turn characteristics

The characteristics of the post-landing turns for the FSC and LCC aircraft are shown in Table 7, defined as the proportion of the total N_T observed turns. The proportion of standard, tight and pivot turns are also visualised in Fig. 16. As for the pre-takeoff taxi phase, it can be seen from Table 7 that the distribution of left and right turns in the post-landing taxi phase is approximately equal. Regarding the FSC fleet, it can be observed that the proportion of pivot and tight turns to standard taxiway turns are consistent with the pre-takeoff taxi phase shown in Table 4, with $\approx$ 85% of post-landing turns being a standard taxiway turn.

It can be observed that Table 7 and Fig. 16 suggest that for the post-landing phase the LCC fleet performs fewer tight and pivot turns compared the FSC fleet, in contradiction to the observations of Section 4.1.1 and the expectation that smaller airport geometries will result in an increased number of tight and pivot turns. This unexpected result is especially highlighted by the LCC aircraft based exclusively at regional airports, which shows the smallest proportion of tight and pivot turns.

However, this observation is expected to be as a result of the degraded ADS-B trajectory quality in the post-landing and turn onto stand phases identified for the LCC fleet, especially for the aircraft operating from regional airports. The ratio of post-landing tight pivot turns observed for the FSC fleet to that of the regional airport based LCC aircraft is 1:1.4, and the ratio of flights containing turn onto stand information between the FSC fleet and the regional airport based LCC aircraft is 1:1.5. These

https://doi.org/10.1017/aer.2024.93 Published online by Cambridge University Press

Table 7. *Post-landing turn characteristics*

Aircraft	N_T	Left	Right	Standard	Tight	Pivot
FSC 1	2,286	50.3%	49.7%	85.6%	13.1%	1.3%
FSC 2	2,331	49.7%	50.3%	86.4%	12.2%	1.4%
FSC 3	2,216	49.6%	50.4%	84.9%	13.4%	1.7%
FSC fleet	*6,833*	*49.9%*	*50.1%*	*85.6%*	*12.9%*	*1.5%*
LCC – large airport	2,411	45.5%	54.5%	89.5%	9.2%	1.3%
LCC – fleet rotation	2,244	48.2%	51.8%	88.8%	9.8%	1.4%
LCC – regional airport	1,696	48.0%	52.0%	89.8%	9.3%	0.9%
LCC fleet	*6,351*	*47.2%*	*52.8%*	*89.4%*	*9.4%*	*1.2%*
Narrow body fleet	13,184	48.6%	51.4%	87.5%	11.2%	1.3%

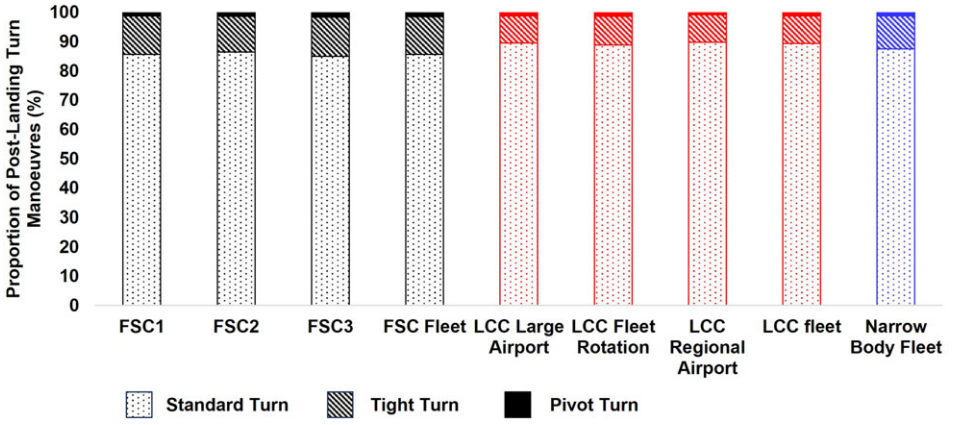

Figure 16. *Proportion of post-landing turn types.*

ratios suggest that the reduced occurrence of tight and pivot turns in the post-landing taxi phase for the LCC fleet is a result of reduced ADS-B trajectory data for the LCC fleet in the post-landing phase, which typically contains tight turn onto stand manoeuvres.

For the fatigue-critical tight and pivot post-landing turn manoeuvres, the turn direction proportions were computed as shown in Table 8. For the post-landing taxi phase, it can again be observed that specific aircraft across the FSC and LCC fleet show a right turn bias for the pivot turn manoeuvres. When coupled with the right tight and pivot turn direction bias for the pre-takeoff taxi phase shown previously in Table 5, it can be suggested that the right-hand main landing gear assemblies of specific aircraft (e.g. FSC 1, FSC 2, and LCC aircraft without fleet rotation) could accumulate fatigue damage at a higher rate than expected compared to the mean rate within the operator and narrow-body fleets.

Finally, Table 9 shows the post-landing turn reversal rate, which can be observed to be lower than the pre-takeoff rate, with approximately a quarter of turning manoeuvres being a turn-reversal across the narrow-body fleet. The impact of airport geometries can be observed within the LCC fleet, with the LCC aircraft under fleet rotation demonstrating increased fatigue-critical turn reversal rates compared to the aircraft based exclusively at regional airports. The latter aircraft is expected to see fewer post-landing turn reversals due to the simpler geometries of smaller regional airports.

4.3 Manoeuvre speeds

The final characteristic of ground manoeuvres during taxi collected within this study concerned the aircraft speed during manoeuvres. The histograms across Fig. 17 show the average and maximum observed

https://doi.org/10.1017/aer.2024.93 Published online by Cambridge University Press

Table 8. *Post-landing tight turn characteristics*

Aircraft	Tight left	Tight right	Pivot left	Pivot right
FSC 1	44.5%	55.5%	34.5%	66.5%
FSC 2	40.0%	60.0%	41.9%	58.1%
FSC 3	43.9%	56.1%	39.5%	60.5%
FSC fleet	*42.8%*	*57.2%*	*38.6%*	*64.1%*
LCC – large airport	50.9%	49.1%	32.3%	67.7%
LCC – fleet rotation	45.9%	54.1%	37.5%	62.5%
LCC – regional airport	53.2%	46.8%	40.0%	60.0%
LCC fleet	*50.0%*	*50.0%*	*36.6%*	*63.4%*
Narrow body fleet	46.4%	53.6%	37.6%	62.4%

Table 9. *Occurrence of post-landing turn reversals*

Aircraft	Post-landing turn reversal rate
FSC 1	26.7%
FSC 2	26.4%
FSC 3	25.8%
FSC fleet	*26.3%*
LCC – large airport	26.4%
LCC – fleet rotation	29.5%
LCC – regional airport	21.9%
LCC fleet	*25.9%*
Narrow body fleet	26.1%

speeds during pre-takeoff and post-landing across the FSC and LCC aircraft fleets. In the vast majority of cases it can be observed that the taxi speeds are consistent across the FSC, LCC and overall narrow-body aircraft fleets. It should be noted that the histogram axes are consistent across Fig. 17 to facilitate direct comparison between individual histograms.

An exception to this is the pre-takeoff taxi speeds between the FSC and LCC fleet, as shown in Fig. 17(a) and 17. The FSC fleet can be observed to have a higher proportion of average taxi speeds $>$ 12kn and maximum taxi speeds greater than $>$ 20kn when compared to the LCC fleet, and this could lead to higher landing gear loading magnitudes for the FSC fleet [1, 4]. Comparing between Fig. 17(a) and (c) infers that average post-landing taxi speeds are higher than average pre-takeoff taxi speeds, as supported by prior FAA loads monitoring campaigns [34, 35].

Another exception concerns the LCC fleet, and in Fig. 17(j) it can be observed that the LCC aircraft based at exclusively large airports demonstrate lower maximum taxi speeds than those observed for the LCC aircraft under fleet rotation and the aircraft based at regional airports. The reduced speeds at larger airports is expected to be as a result of congestion at larger airports, which could to aircraft queuing at runway hold points and lower achievable taxi speeds.

Finally, Fig. 18 shows the histograms relating to the average aircraft ground speeds observed across the turning manoeuvres extracted from the flights across FSC and LCC fleets. From across Fig. 18 it can be observed there is little difference between the mode average turn speeds and variability across the FSC and LCC fleets and individual aircraft. From comparing Fig. 18(a) and (b) it can be seen that the average speed during post-landing turns is approximately 2kn higher than turns performed during the pre-takeoff taxi phase.

https://doi.org/10.1017/aer.2024.93 Published online by Cambridge University Press

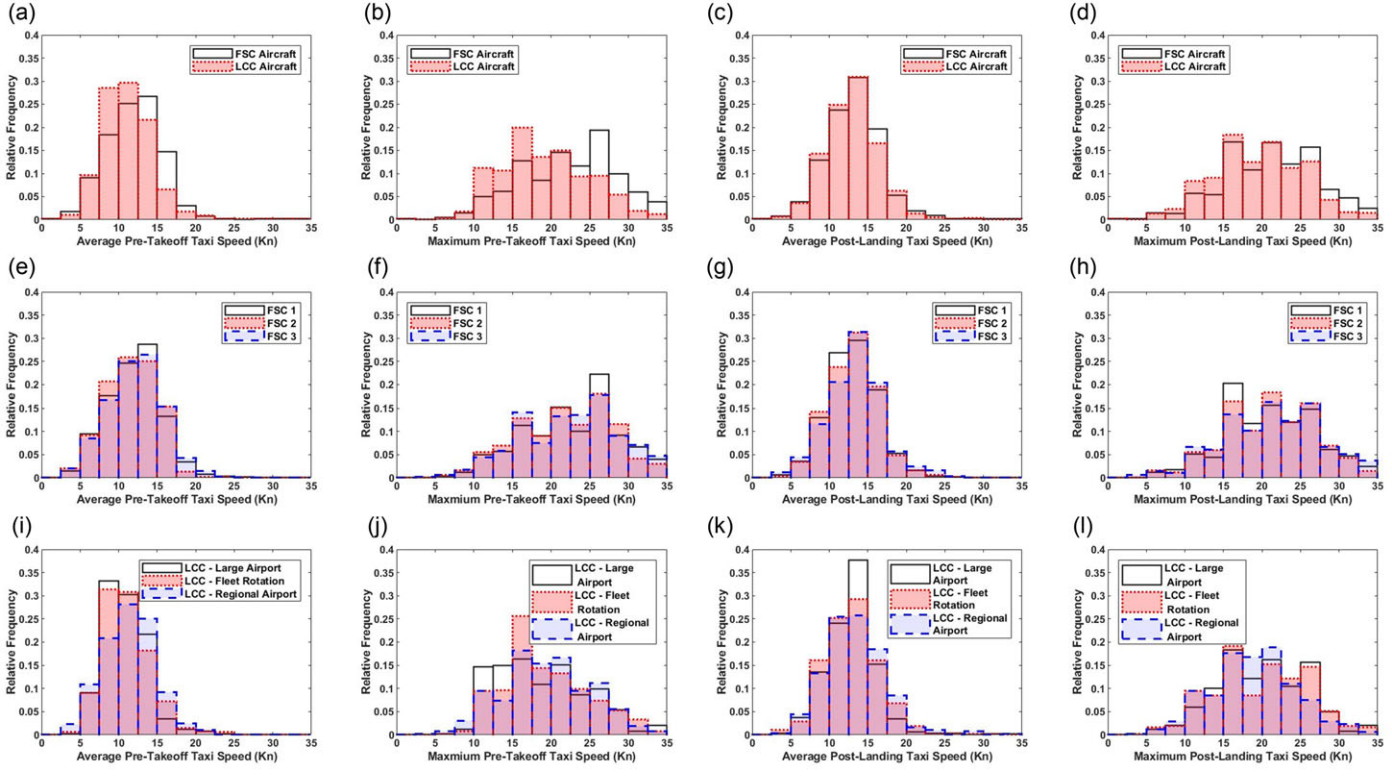

Figure 17. *Taxi speed statistics: fleet-level (a) average and (b) maximum pre-takeoff taxi speed, (c) average and (d) maximum post-landing taxi speed, full-service carrier (e) average and (f) maximum pre-takeoff taxi speed, (g) average and (h) maximum post-landing taxi speed and low-cost carrier (i) average and (j) maximum pre-takeoff taxi speed, (k) average and (l) maximum post-landing taxi speed.*

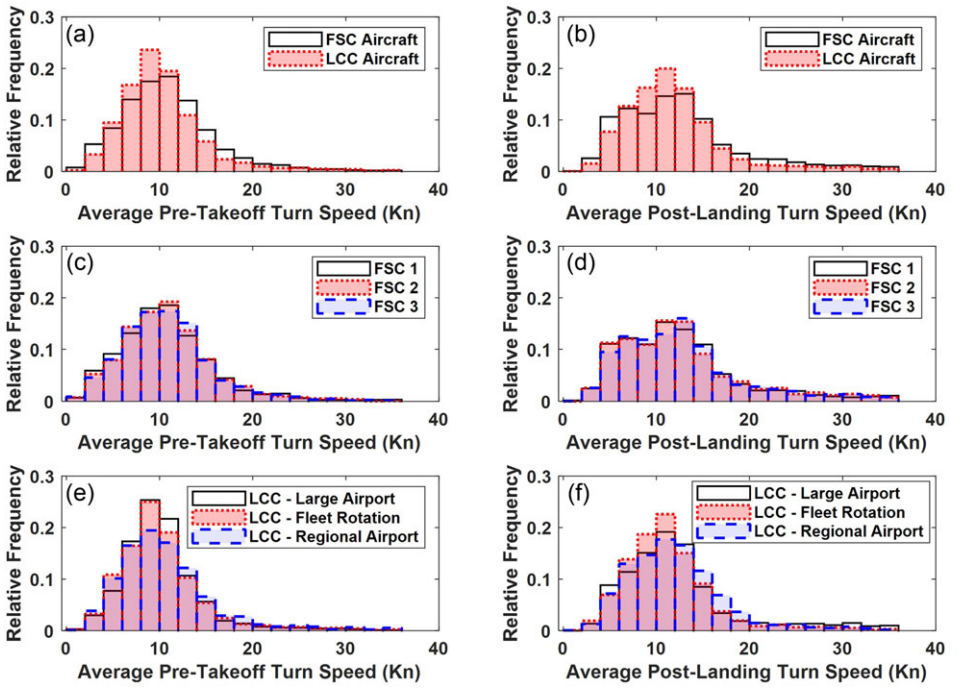

Figure 18. *Ground speed during turns statistics: fleet-level (a) pre-takeoff and (b) post-landing average speed during turns, full-service carrier (c) pre-takeoff and (d) post-landing average speed during turns and low-cost carrier (e) pre-takeoff and (f) post-landing average speed during turns.*

4.4 Further operator characteristics

To further explore the impact of operator characteristics and inform future studies, an additional operator characteristic of ultra-low-cost carrier (ULCC) was identified to have a potential impact on landing gear ground manoeuvres due to their extensive use of secondary airports within their route networks [36]. A single narrow-body airframe from a European ULCC was identified and the ADS-B trajectories for the flights in June 2023 (170 flights) were sourced from Flightradar24 [24] and processed using the methodology described in Section 2. The histograms shown in Figs. 19 and 20 compare the ULCC airframe turning manoeuvre occurrences, taxi distances and manoeuvre speeds with the aggregated FSC fleet and LCC fleet values. The reliance on secondary airports is evident in the reduced mode number of pre-takeoff turns (Fig. 19(a)), pre-takeoff taxi distance (Fig. 19(b)) and post-landing taxi distance (Fig. 19(c)) compared to the FSC and LCC fleets. These histograms can therefore initially suggest that the occurrence of fatigue loads on landing gear assemblies is lower, due to reduced loading occurrences from turns and bump loads during taxi.

However, within Fig. 20(a), (f) and (e) it can be observed that the ULCC airframe demonstrated increased levels of ground speed during pre-takeoff taxi and turns, often exceeding the speeds observed for the FSC fleet. For example, Fig. 20(e) indicates that the average ground speed during a turn exceeds 12kn in 45% of ULCC pre-takeoff turns, compared to 32% and 23% for the FSC and LCC fleets, respectively. The observed increased in manoeuvre speeds suggests that whilst the ULCC aircraft landing gear is exposed to fewer ground manoeuvres, the loads occurring during these manoeuvres may be higher.

The characteristics of the pre-takeoff turns performed by the ULCC aircraft are given in Table 10, with the proportions of standard, tight and pivot turns visualised in Fig. 21. It can be observed that the ULCC aircraft has a similar occurrence of tight and pivot turns to the LCC fleet, albeit with increased rates of pivot turns, approaching double that of the FSC fleet. In addition a bias towards left-hand tight

https://doi.org/10.1017/aer.2024.93 Published online by Cambridge University Press

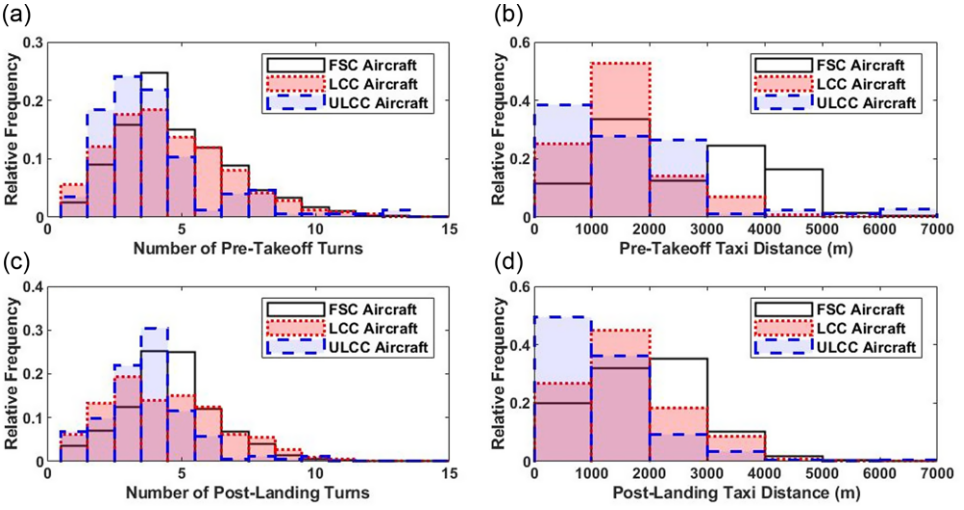

Figure 19. *Comparison of full-service carrier fleet, low-cost carrier fleet and ultra-low-cost carrier aircraft ground manoeuvre statistics: (a) pre-takeoff turn occurrence, (b) pre-takeoff taxi distance, (c) post-landing turn occurrence, (d) post-landing taxi distance.*

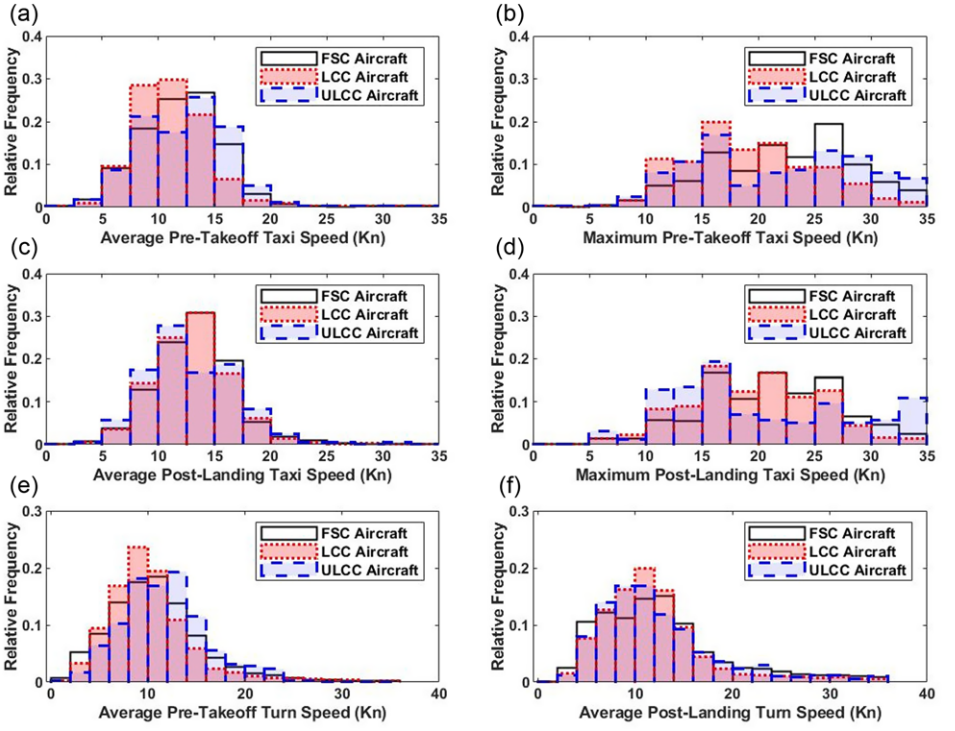

Figure 20. *Comparison of full-service carrier fleet, low-cost carrier fleet and ultra-low-cost carrier aircraft ground manoeuvre statistics: (a) average pre-takeoff taxi speed, (b) maximum pre-takeoff taxi speed, (c) average post-landing taxi speed, (d) maximum post-landing taxi speed, (e) average pre-takeoff ground speed during turns and (f) average post-landing ground speed during turns.*

https://doi.org/10.1017/aer.2024.93 Published online by Cambridge University Press

Table 10. *Pre-takeoff turn characteristics for ULCC*

	Proportion of turn manoeuvres		
Turn type	ULCC	FSC	LCC
Standard	82.0%	87.4%	81.1%
Tight	13.7%	10.1%	15.8%
Tight Left	*8.8%*	*5.2%*	*6.9%*
Tight Right	*4.9%*	*4.9%*	*8.9%*
Pivot	4.3%	2.5%	3.1%
Pivot Left	*2.5%*	*1.0%*	*1.5%*
Pivot Right	*1.8%*	*1.5%*	*1.6%*
Turn reversal	26.0%	30.5%	32.1%

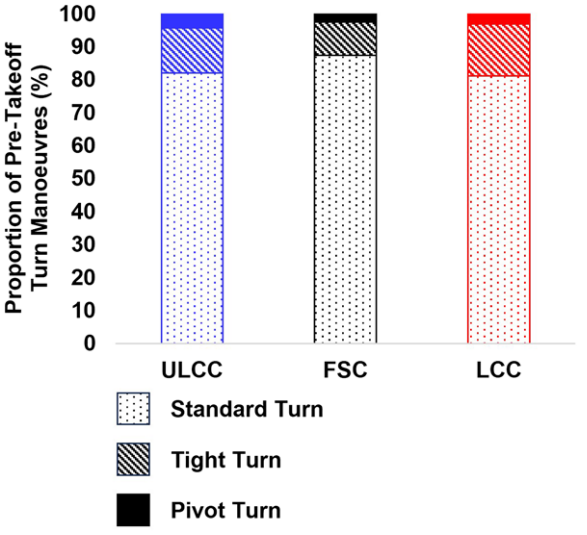

Figure 21. *Pre-takeoff turn proportions across operator fleets.*

and pivot turns can be observed for the ULCC aircraft from Table 10. These results suggest a higher rate of fatigue-critical tight turns occur for the ULCC aircraft. It is interesting to note however, that the routes operated by the ULCC aircraft lead to a reduced occurrence of fatigue-critical turn reversals, in contradiction to the observations in Table 6. The post-landing turn characteristics are shown in Table 11 and again, the increased occurrence of pivot turns (as also shown in Fig. 22), but reduced occurrence of turn-reversals can be observed.

5.0 Discussion

The most pertinent results from the previous section are shown in Table 12 and demonstrate that the ground manoeuvres that aircraft perform, and subsequent loading occurrences and magnitude applied to aircraft landing gear, are intrinsically linked to the characteristics of the aircraft operator as a result of the size and geometry of the airports that the operator has within its route network. At a high level, this has been demonstrated through the observation that for a fleet of FSC aircraft based at the same large international airport that their ground manoeuvre occurrences and characteristics were consistent across the three individual aircraft, whilst the LCC aircraft fleet not only showed differences in manoeuvre

https://doi.org/10.1017/aer.2024.93 Published online by Cambridge University Press

Table 11. *Post-landing turn characteristics for ULCC*

	Proportion of turn manoeuvres		
Turn type	ULCC	FSC	LCC
Standard	86.6%	85.6%	89.4%
Tight	10.7%	12.9%	9.4%
Tight Left	*6.2%*	*5.5%*	*4.7%*
Tight Right	*4.5%*	*7.4%*	*4.7%*
Pivot	2.7%	1.5%	1.2%
Pivot Left	*1.2%*	*0.6%*	*0.4%*
Pivot Right	*1.5%*	*0.9%*	*0.8%*
Turn reversal	22.1%	26.3%	25.9%

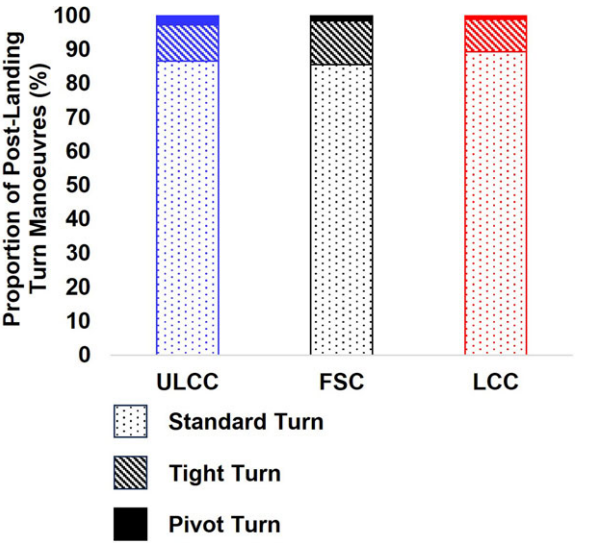

Figure 22. *Post-landing turn proportions across operator fleets.*

occurrence and characteristics when compared to the FSC fleet, but also between each of the individual LCC aircraft.

As an overall summary, as airport size reduces, the occurrence of turning manoeuvres reduces along with the required pre-takeoff and post-landing distances. In addition, the proportion of tight and pivot turns during the pre-takeoff taxi phase increases as the airport size reduces. As LCC carriers will typically operate route networks reliant on small secondary and regional airports [32], they should be expected to see ground manoeuvre occurrences that differ from those of an FSC based at large international airports. A key observation from the presented study concerns the difference in the proportion of turns found to be tight or pivot turns during the pre-takeoff taxi phase, at ≈15% for the FSC fleet and 20% for the LCC fleet. Based on the observed mode number of pre-takeoff turns of four for the FSC and LCC fleets (see Fig. 12 previously), this would lead to six and eight tight or pivot turns being performed on average every 10 flights for an FSC and LCC aircraft respectively. As this represents that an LCC aircraft would be a performing a third more fatigue-critical tight turning manoeuvres, leading to increased fatigue damage accumulation, it can be observed that fatigue spectra aligned to the operator characteristics may need to be considered. Such a consideration may be especially necessary as such manoeuvres are performed at higher pre-takeoff aircraft masses. When the same calculation process is

https://doi.org/10.1017/aer.2024.93 Published online by Cambridge University Press

Table 12. *Summary of results across aircraft operators*

Manoeuvre statistics	FSC fleet	LCC fleet	ULCC aircraft
Mode pre-takeoff turns	4	4	3
Mode pre-takeoff taxi distance (m)	1,500	1,500	500
Mode post-landing turns	4	3	4
Mode post-landing taxi distance (m)	2,500	1,500	500
Mode pre-takeoff turn speed (Kn)	11	9	13
Average number of pre-takeoff Tight/pivot turns per 10 flights	6	8	6

applied to the limited data from the ULCC aircraft, it can be observed that the aircraft performs on average six tight or pivot turns for every 10 flights. The higher observed rate of fatigue-critical turns for the ULCC airframe is offset by the lower mode number of pre-takeoff turns (see Table 12). Unfortunately, currently assumed rates of tight and pivot turns within landing gear load spectra are not publicly available, so it is unclear whether the identification of in-service tight turn occurrences in relation to operator characteristics would support a reduction in spectra conservatism or support the development of more representative spectra for fatigue design.

However, of greater significance to landing gear design, operation and maintenance are that the results presented in Section 4 have highlighted that even beyond the level of operator characteristics, there can be notable airframe-to-airframe variability within an operator fleet. The clear ground manoeuvre trends across the LCC fleet that relate to the aircraft base type show that an assumed fatigue loading spectrum across the entire fleet would not capture the complexity of the operator's route network and fleet rotation strategy, and hence may not be representative for all airframes within the fleet. This observation further supports the adoption of landing gear structural health monitoring systems, which has achieved growing coverage within the literature [14, 17, 18]. As development of structural health monitoring systems and practices can require significant resources [28], a more immediate use of the methodology and results presented in this study could be to support the identification of specific operator characteristics or airframes to consider during the development of such approaches, as previously considered in prior work concerning helicopter usage monitoring [27, 28].

The need for structural health monitoring of aircraft landing gear is further highlighted by considering the characteristics of the pre-takeoff tight turns shown previously in Table 5, where it was observed that specific airframes were biased towards certain tight turn directions, potentially leading to increased fatigue damage accumulation within specific main landing gear assemblies (i.e. left or right-hand main landing gear). These observations demonstrate that rather than performing structural health monitoring at an airframe level, it must also be performed at a landing gear assembly level. It is also important to note that this study has only considered the variability in the occurrence of manoeuvres, rather than the significant variability observed in the magnitude of landing gear loads [11, 34, 35]. The known loading magnitude variability for landing gear ground manoeuvres provides further justification for investigation into landing gear structural health monitoring techniques.

It is important to highlight that the ULCC results shown in Section 4.4 only consider a single airframe over a limited period of operation and consequently, the above results may differ and converge towards the LCC fleet characteristics if multiple ULCC aircraft were investigated for the 500 flight timeframe employed for the other fleets. Regardless, these results have highlighted further justification for structural health monitoring of landing gear assemblies, as the ULCC aircraft presents the situation where a reduced number of load occurrences are observed, but with the potential for greater load magnitudes within those occurrences. The impact on the fatigue life of such operational characteristics could only be ascertained through fatigue analysis of the observed spectrum, or through structural health monitoring.

https://doi.org/10.1017/aer.2024.93 Published online by Cambridge University Press

Table 13. *Proportion of dataset containing taxi route elements for 2023 data*

Aircraft	Pushback	Pre-takeoff	Post-landing	Turn onto stand	Complete taxi
FSC 1 2023	93.1%	96.6%	90.3%	86.2%	79.3%
LCC 1 2023	82.1%	87.1%	85.0%	72.0%	55.7%
Narrow body fleet 2023	87.6%	91.9%	87.3%	87.7%	67.5%

6.0 Limitations, outlook and future work

The current limitations with the proposed study can be decomposed into the accuracy of the manoeuvre characterisation, the quality of the ADS-B trajectory data and constraints within the collected data for the FSC and LCC fleets.

Firstly, whilst the enhanced turn characterisation algorithm showed that it was able to correctly identify the full taxi route in 77% of flights compared to the 50% success rate achieved in prior work [6], it is clear that the robustness of the algorithms still needs to be refined. For example, flights demonstrated errors in the pre-takeoff taxi phase propagated from incorrect pushback characterisation, which originates in the noisy ADS-B data observed at stand and gate locations [6]. Further investigation into how ground manoeuvre characterisation can be made robust to this lower-quality ADS-B data and propagation of errors needs to be investigated as a priority. Errors during the post-landing phase were typically due to missing or 'jumps' in the ADS-B trajectory data, and again, further work is required to increase the robustness of the ground manoeuvre characterisation algorithms, despite the significant improvement achieved over the original methodology presented in prior work [6].

It can therefore be seen that the accuracy of ground manoeuvre identification from ADS-B trajectories is inherently linked to the quality of the ADS-B trajectory data. To explore whether data quality had improved since the 2021 data collection timeframe, one aircraft from the FSC and LCC fleets was selected and ADS-B trajectories for one month of operation during Spring 2023 were sourced from Flightradar24 [24]. It was found the LCC aircraft based at a large airport during the study had now entered a fleet rotation phase, highlighting the complexity of operator route networks and fleet rotation strategy. For the 146 FSC and 140 LCC aircraft flights, the ADS-B trajectories were visually assessed for containing taxi route elements as described previously in Section 3.1. The resulting occurrences of taxi route elements in the 2023 data are given in Table 13.

From comparing Tables 1 and 13, it can be observed for the FSC aircraft that there is an increase in flights containing pre-takeoff and post-landing taxi routes by 5%, leading to a nearly 10% increase in the number of FSC flights showing the complete taxi route. Pushback and turn onto stand elements remained consistent with the 2021 dataset. The LCC fleet on the other hand shows limited change in data completeness between 2021 and 2023 datasets, with less than a 5% increase in the number of flights showing the complete taxi routes. At the narrow-body fleet level, a 4% increase in the number of flights with complete taxi routes has been observed over the two-year window.

When compared to 2019 data used in a prior study on wide-body aircraft [6], it is suggested that ADS-B coverage for aircraft ground operations increases by approximately 2% of flights a year, although this will be highly sensitive to the global location and airports served by aircraft due to the current reliance on crowd-sourced data from ground receivers. However, with ADS-B set to become a cornerstone technology for air traffic control and air traffic management [25], there is the potential for a rapid increase in the coverage and quality of ADS-B derived ground trajectories in conjunction with such data being sourced from a certified, rather than predominately enthusiast or research-led source. When coupled with 'map-matching' algorithms that have been recently developed to enable ADS-B ground trajectories to be linked to known airport geometries [37], ADS-B may continue to evolve into a robust data source for aerospace system design and monitoring. There is also the potential future synthesis of such approaches with aggregated data of aircraft ground trajectories to support the simulation and optimisation of aircraft trajectories at airports as considered by Ma et al. [38].

https://doi.org/10.1017/aer.2024.93 Published online by Cambridge University Press

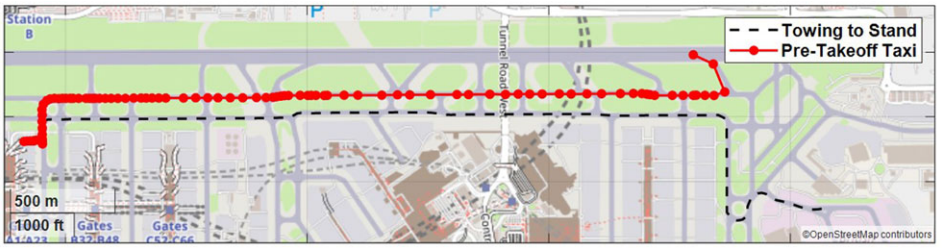

Figure 23. *Example of towing trajectory pior to pre-takeoff taxi. ADS-B data from Flightradar24 [24]. Map data from OpenSteetMap (https://www.openstreetmap.org/copyright).*

The collected dataset also contains limitations when attempting to generalise operator characteristics on landing gear ground manoeuvres. Firstly, the data collection window equal to the approximate timeframe between heavy maintenance checks of 500 flights only represented approximately six months of operation. A longer data collection window would be required to capture all aspects of an operator's route network, and any fleet rotation strategies employed, as observed for the LCC aircraft that during 2021 was based predominately at a large airport being subject to fleet rotation in 2023. The data collection window of Summer-Autumn 2021 may have also captured non-standard route networks for operators recovering from the COVID-19 pandemic [22].

Another limitation of the collected dataset was that whilst both the FSC and LCC were European-based operators, the aircraft considered were all based at airports within the same country. This limitation could lead to the aircraft across the two fleets operating on similar routes, leading to a reduction in the impact of the operator characteristics on ground manoeuvres. Future work should endeavour to also consider the impact of geographical characteristics of operators, through investigating aircraft not just from European fleets, but global fleets. A wider consideration of other FSC operators would also provide insight as to whether fleet rotation around various large international airport bases impacts ground manoeuvre occurrence, as the FSC fleet within this study were consistently based at a large international airport. In addition, the initial study into ground manoeuvres of an ULCC aircraft in Section 4.4 highlights the need to study ULCC aircraft fleets further. These limitations of the dataset presented in this paper provide the natural follow-on and future work concerning the exploitation of ADS-B trajectories for characterising aircraft ground manoeuvres. Ultimately, such a comprehensive study could support the construction of bespoke fatigue spectra related to operator business and geographical characteristics, leading to more efficient and if required, more reliable, landing gear structures and systems.

Concerning future work, the collected ADS-B trajectories has highlighted significant landing gear focused opportunities. Within on-going work, ADS-B trajectories containing taxi routes related to towing the aircraft from maintenance/remote parking to the departure gate (see Fig. 23) have been observed. The towing portion of the trajectory could be segregated from the pre-takeoff taxi due to the significant duration observed between the towing and pre-takeoff taxi sections due to preparations for flight and boarding. Fatigue loads applied to aircraft landing gear are known to be significantly different under towing operations, especially for the nose landing gear [1, 4] and consequently, ADS-B trajectories may provide a route to better characterising the manoeuvres performed during aircraft towing. In addition, the increasing number of regional aircraft now fitted with ADS-B transponders [39] will permit ground manoeuvre occurrences for such aircraft to also be investigated, permitting comparison across regional, narrow-body and wide-body aircraft. A recent example of the exploitation of ADS-B ground trajectories for regional aircraft concerns the derivation of electric taxiing requirements for regional aircraft presented by Taltaud et al. [40].

Finally, whilst this paper has considered landing gear specifically, the continual and evolving utilisation of ADS-B data in the area of structural health monitoring highlights future opportunities for

https://doi.org/10.1017/aer.2024.93 Published online by Cambridge University Press

aerospace structures and systems in general. Of current interest to the authors is the exploration of inferring airframe loads from ADS-B data [30], which could facilitate the remote monitoring of aircraft structures based upon air traffic data.

7.0 Conclusions

The ground manoeuvres performed by aircraft are intrinsically linked to the airport geometries from which they operate in-service. Consequently, the characteristics of an aircraft operator are anticipated to impact the various cyclic loads that the landing gear is subjected to during taxi. Without widespread structural health monitoring, landing gear fatigue design and substantiation is reliant on an assumed fleet-wide fatigue load spectrum, potentially leading to design conservatism or un-representative fatigue design assumptions. This paper has presented the enhanced characterisation of ground turning manoeuvres within ASD-B air traffic data. In order to quantify the impact of aircraft operator characteristics on the occurrence of landing gear ground manoeuvres, the enhanced ADS-B turn manoeuvre characterisation algorithm was applied to 500 flights of three FSC aircraft and three LCC aircraft. The characterisation of the ADS-B trajectory data and observed manoeuvres led to the following conclusions:

- Characterisation of turning manoeuvres based on ADS-B latitude and longitude rather than reported aircraft track information increased the rate of successfully identifying a complete set of aircraft taxi manoeuvres by ≈30%.
- The availability of ground ADS-B trajectories is increasing at approximately 2% of flights per year.
- During the pre-takeoff taxi phase, the FSC aircraft fleet showed consistent turning manoeuvre occurrences, whilst the LCC fleet demonstrated differences in the mode number of turning manoeuvres and variability in taxi distance.
- When comparing the FSC fleets and LCC fleets, the mode number of pre-takeoff turns was found to be the same, but there was significant differences in the pre-takeoff taxi distances between different aircraft.
- During the post-landing taxi phase, significant differences in the number of turn occurrences and taxi distances were observed between the LCC aircraft and when comparing the FSC aircraft fleet and LCC aircraft fleet as a whole.
- Regarding fatigue-critical tight and pivot turns, it was observed that the LCC aircraft performed a larger number of tight and pivot turns, where for every 10 flights the LCC aircraft performed on average eight tight or pivot turns, compared to the six observed for the FSC aircraft fleet.
- Further characterisation of the tight and pivot turns showed that specific aircraft across the FSC and LCC fleets biased such manoeuvres towards a specific turn direction. This observation suggests an increased fatigue damage accumulation rate in specific main landing gear assemblies (e.g. the right-hand side main landing gear of individual aircraft).

The findings of this paper support the need for further investigations into landing gear fatigue load spectra that better reflect the characteristics of aircraft operators. The development of such load spectra could lead to a challenge of existing design conservatism, ultimately reducing component masses or extending component lives, whilst still ensuring landing gear assemblies retain their structural integrity in-service. The results from the presented case study, along with an initial investigation into the taxi speeds during manoeuvres for an aircraft operated by an ULCC, has also provided support for the growing interest in structural health monitoring for aircraft landing gear, due to the complex coupling of manoeuvre occurrence and loading magnitude when assessing the fatigue damage accumulation within individual landing gear assemblies.

Finally, this paper has highlighted current limitations around robustly identifying and segregating pushback manoeuvres with ADS-B trajectories, along with discussing future exploitation of the

https://doi.org/10.1017/aer.2024.93 Published online by Cambridge University Press

presented methodology across a wider dataset, that could encompass global variations in operator characteristics and characterising the ground manoeuvre occurrences of regional aircraft.

Acknowledgements. This paper presents work performed as part of the Aerospace Technology Institute (ATI) funded 'Optimised Life for Landing Gear Assemblies (OLLGA)' Project (grant no. 10040817) in collaboration with Safran Landing Systems. The authors extend their personal thanks to FlightRadar24® for providing permission to reproduce ADS-B data within this paper. Presented maps in Figs. 1–7 and 23 are generated from Map data from OpenSteetMap (https://www.openstreetmap.org/copyright).

Competing interests. The authors declare none.

References

[1] Buxbaum, O. Landing gear loads of civil transport aircraft, Aircraft Fatigue in the Eighties - Proceedings of the ICAF-Symposium, 1981.
[2] Federal Aviation Administration DOT/FAA/AR-02/129 - Side Load Factor Statistics From Commercial Aircraft Ground Operations, 2003.
[3] El Mir, H. and Perinpanayagam, S. Certification of machine learning algorithms for safe-life assessment of landing gear, *Front. Astronomy Space Sci.*, 2022, **9**, pp 1–16.
[4] Ladda V. and Struck, H. Operational loads on landing gear, Landing Gear Design Loads - AGARD Conference Proceedings CP484, 1990.
[5] Schmidt, R.K. Is 'Safe-Life' Safe Enough?, 2017, MSc, Cranfield University.
[6] Hoole, J., Sartor, P., Booker, J.D., Cooper, J.E., Gogouvitis, X.V. and Schmidt, R.K. Landing gear ground manoeuvre statistics from automatic dependent surveillance-broadcast transponder data, *Aeronaut. J.*, 2021, **125**, (1293), pp 1942–1976.
[7] Sartor, P., Bond, D.A., Staszewski, W.J. and Schmidt, R.K. Value of an overload indication system assessed through analysis of aviation occurrences, *J. Aircraft*, 2009, **46**, (5), pp 1692–1705.
[8] Hoole, J. Probabilistic Fatigue Methodology for Aircraft Landing Gear, 2020, PhD, University of Bristol.
[9] Air Accident Investigations Branch Report on the accident to McDonnell-Douglas MD-83 EC-FXI at Liverpool Airport on 10 May 2001, 2003.
[10] Cavallini, G. and Lazzeri, R. A probabilistic approach to fatigue risk assessment in aerospace components, *Eng. Fract. Mech.*, 2007, **74**, pp 2964–2970.
[11] Sartor, P., Becker, W., Worder, K., Schmidt, R.K. and Bond, D. Bayesian sensitivity analysis of flight parameters in a hard-landing analysis process, *J. Aircraft*, 2016, **53**, (5), pp 1317–1331.
[12] Holmes, G., Sartor, P., Reed, S., Southern, P., Worden, K. and Cross, E. Prediction of landing gear loads using machine learning techniques, *Struct. Health Monit.*, 2016, **15**, (5), pp 568–582.
[13] Petrone, G., Bruno, M., Bocchetto, F., Breglio, G., Pugliese M., Caldara, A., Nocella, A., Cavallari, A., Schiano lo Moriello, S., Capuano, G. and Rossetti, D. An innovative health monitoring system for aircraft landing gears, 8th European Workshop on Structural Health Monitoring (EWSHM 2016), 5-8 July 2016, Bilbao, Spain.
[14] Forrest, C., Forrest C. and Wiser, D. Landing gear Structural Health Monitoring (SHM), 2nd International Conference on Structural Integrity (ICSI 2017), 4-7 September 2017, Funchal, Maderia, Portugal.
[15] Skorupka, Z. and Tywoniuk, A. Health monitoring in landing gears, *J. KONES Powertrain Transp.*, 2019, **26**, (1), pp 1–8.
[16] Dziendzikowski, M., Kurnyta, A., Reymer, P., Kurdelski, M., Klysz, S., Leski, A. and Dragan, K. Application of operational load monitoring systems for fatigue estimation of main landing gear attachment frame of an aircraft, *Materials*, 2021, **14**, (6564), 1–20.
[17] Fu, Y., Fu, H. and Zhang, S. A novel safe life extension method for aircraft main landing gear based on statistical inference of test life data and outfield life data, *Symmetry*, 2023, **15**, (880), pp 1–14.
[18] Skorupka, Z. and Liao, M. Review of aircraft landing gear tests as part of structural testing, 31st International Committee on Aeronautical Fatigue and Structural Integrity (ICAF) Symposium, 26-29 June 2023, Delft, The Netherlands.
[19] Corrado, S.J., Puranik, T.G. and Mavris, D.N. Characterising terminal airspace operational states and detecting airspace-level anomalies, *Eng. Proc.*, 2021, **13**, (1), pp 1–9.
[20] Schultz, M., Olive, X., Rosenow, J., Fricke, H. and Alam, S. Analysis of airport ground operations based on ADS-B data, 2020 International Conference on Artificial Intelligence and Data Analytics for Air Transportation (AIDA-AT), 3-4 February, 2020, Singapore.
[21] Sun, J., Basora, L., Olive, X., Strohmeier, M., Schäfer, M., Martinovic, I. and Lenders, V. OpenSky Report 2022: evaluating aviation emissions using crowdsourced open flight data, IEEE/AIAA 41st Digital Avionics Systems Conference (DASC), 18-22 September 2022, Portsmouth, VA, USA.
[22] Sun, J., Olive, X., Strohmeier, M., Schäfer, M., Martinovic, I. and Lenders, V. OpenSky Report 2021: insights on ADS-B mandate and fleet deployment in times of crisis, IEEE/AIAA ${40^{st}}$ Digital Avionics Systems Conference (DASC), 3-7 October 2021, San Antonio, TX, USA.
[23] Sun, J. *The 1090 Megahertz Riddle: A Guide to Decoding Mode S and ADS-B Signals*, 2nd ed, 2021, TU Delft OPEN Publishing.
[24] Flightradar24, https://www.flightradar24.com [accessed 8th August 2023].

https://doi.org/10.1017/aer.2024.93 Published online by Cambridge University Press

[25] Schäfer, M., Strohmeir, M., Lenders, V., Martinovic, I. and Wilhelm, M. Bringing up Opensky: a large-scale ADS-B sensor network for research, 13th IEEE/ACM International Symposium on Information Processing in Sensory Networks (IPSN), 2014, pp 83–94.
[26] Ali, B.S., Schuster, W., Ochieng, W. and Majumdar, A. Analysis of anomalies in ADS-B and its GPS data, *GPS Solutions*, 2016, **20**, pp 429–438.
[27] Hoole, J., Booker, J.D. and Cooper J.E. Helicopter flight manoeuvre statistics via ADS-B: an initial investigation using the OpenSky network, *Eng. Proc.*, 2021, **13**, (1), pp 1–10.
[28] Hünemohr, D., Litzba, J. and Rahmimi, F. Usage monitoring of helicopter gearboxes with ADS-B flight data, *Aerospace*, 2022, **9**, (11), pp 1–17.
[29] Meyer, H., Zimdahl, J., Kamtsiuris, A., Meissner, R., Raddatz, F., Haufe, S. and Bäßler, M. Development of a digital twin for aviation research, *Deutscher Luft- und Raumfahrtkongress,* 2020.
[30] Hoole, J., Booker, J.D., Cooper, J.E. and Richardson, T.S. Remote sensing of aerospace usage profiles via air traffic data, *Review of Aeronautical Fatigue and Structural Integrity Investigations in the UK During the Period May 2021-April 2023*, Hallam, D. (Ed), 2023.
[31] Federal Aviation Administration AC150/5300-13B - Airport Design, 2022.
[32] Graham, A. Understanding the low cost carrier and airport relationship: A critical analysis of the salient issues, *Tourism Manage.*, 2013, **36**, pp 66–76.
[33] Andrade, P., Silva, C., Ribeiro, B. and Santos, B.F. Aircraft maintenance check scheduling using reinforcement learning, *Aerospace*, 2021, **8**, (113).
[34] Federal Aviation Administration DOT/FAA/AR-98/28 - Statistical Loads Data for Boeing 737-400 Aircraft in Commercial Operations, 1998.
[35] Federal Aviation Administration DOT/FAA/AR-02/35 - Statistical Loads Data for the Airbus A-320 Aircraft in Commercial Operations, 2002.
[36] Taplin, D., Kuby, M., Salon, D. and King, D., Analysis of airports served by ultra low-cost carriers, J. Transp. Res. Board, 2023, *in press*.
[37] Szymanski, M., Ghazi, G. and Botez, R.M. Development of a map-matching algorithm for the analysis of aircraft ground trajectories using ADS-B data, AIAA Aviation 2023 Forum, 12-16 June 2023, San Diego, CA, USA.
[38] Ma, J., Zhou, J., Liang, M. and Delahaye, D. Data-driven trajectory-based analysis and optimization of airport surface movement, *Transp. Res. Part C*, 2022, **145**, pp 1–20.
[39] Jux, B., Foitzik, S. and Doppelbauer, M. A standard mission profile for hybrid-electric regional aircraft based on web flight data, 2018 IEEE International Conference on Power Electronics, Drives and Energy Systems (PEDES), 18-21 December 2018, Chennai, India.
[40] Taltaud, A., Carbonneau-Côté, J., Bouchard, M. and Rancourt, D. Statistical approach for electric taxiing requirements for regional turboprop aircraft, J. Aircraft, 2023, *in press*.

Cite this article: Hoole J., Booker J.D. and Cooper J.E. (2024). Impact of operator characteristics on landing gear ground manoeuvre occurrences. *The Aeronautical Journal*, **128**, 2604–2633. https://doi.org/10.1017/aer.2024.93